

DisQ: A Markov Decision Process Based Language for Quantum Distributed Systems

LE CHANG, University of Maryland, USA
SAITEJ YAVVARI, Iowa State University, USA
RANCE CLEVELAND, University of Maryland, USA
SAMIK BASU, Iowa State University, USA
LIYI LI, Iowa State University, USA

The development of quantum computers has reached a great milestone, in spite of restrictions on important quantum resources: the number of qubits being entangled at a single-location quantum computer. Recently, there has been some work to combine single-location quantum computing and quantum networking techniques to develop distributed quantum systems such that large entangled qubit groups can be established through remote processors, and quantum algorithms can be executed distributively. We present DisQ as a framework to facilitate the rewrites of quantum algorithms to their distributed versions. The core of DisQ is a distributed quantum programming language that combines the concepts of Chemical Abstract Machine (CHAM) and Markov Decision Processes (MDP) with the objective of providing a clearly distinguishing quantum concurrent and distributed behaviors. Based on the DisQ language, we develop a simulation relation for verifying the equivalence of a quantum algorithm and its distributed versions. We present several case studies, such as quantum addition and Shor's algorithm, to demonstrate their equivalent rewrites to distributed versions.

1 INTRODUCTION

Quantum computing development has shown a great potential for quantum advantage to program substantially faster algorithms compared to those written for classical computers, e.g., Shor's algorithm [Shor 1994] can factor a number in polynomial time, even though this problem is not known to be polynomial-time-computable in the classical setting. However, near-term intermediate-scale quantum (NISQ) computers have scalability challenges in executing practical quantum applications [Caleffi et al. 2022]. Quantum qubit entanglement, a major resource utilized in quantum algorithms, becomes the major bottleneck because a single-location NISQ computer usually has a fixed maximum of the allowed entangled qubit number due to machine limitations. Such limitations cannot be mitigated by single-location parallelism and concurrency. Hence, quantum teleportation-based remote location quantum networking techniques have been experimented with in recent years to distributively execute quantum algorithms [Caleffi et al. 2022; Tang and Martonosi 2024]. The key idea is combining the two techniques to create large entangled qubit groups and mitigate the scalability challenge.

Existing quantum circuit-based programming languages [Feng et al. 2012; Gay and Nagarajan 2005; Ying and Feng 2009] focus on developing quantum parallelism and concurrency that can be used for simulating quantum distributed systems but do not explicitly support the specification of the quantum distributed deployment mechanism. Below, we summarize the distinguishing aspects of different quantum concurrent and distributed models.

- Quantum *concurrency* provides a high-level abstraction of partitioning a quantum sequential program into different subparts, which can be executed concurrently. Here, *parallelizing* a quantum program refers to the different subpart executions that do not communicate with each other, while *concurrent* execution means that different subparts might communicate through qubit information sharing.

Authors' addresses: Le Chang, University of Maryland, USA, lchang21@umd.edu; Saitej Yavvari, Iowa State University, USA, saitej02@iastate.edu; Rance Cleaveland, University of Maryland, USA, rance@cs.umd.edu; Samik Basu, Iowa State University, USA, sbasu@iastate.edu; Liyi Li, Iowa State University, USA, liyili2@iastate.edu.

- A *distributed* quantum programming modeling, on the other hand, takes into account the machine limitations when combining different techniques for constructing distributed systems and tries to reflect the exact program behaviors in a remote location quantum programming environment.

Simulating a quantum distributed system through a single-location quantum concurrency model may misrepresent some key features in combining the quantum circuit and networking techniques. For example, qubits in a single location cannot be a message transmitted to remote locations or manipulated by operations in remote locations, as the only way to communicate the information in these qubits is through quantum networking techniques. In addition, a defined distributed quantum program must respect its original sequential program behavior, which requires a mechanism to verify such sequential to distributed program rewrites.

To properly enable rewriting sequential quantum programs to corresponding distributed versions, we propose `DisQ`, a programming language formalism inspired by the classical *Chemical Abstract Machine* [Berry and Boudol 1992] (CHAM), permitting the definitions, distinctions, and analyses of both concurrent and remotely distributed quantum programs. `DisQ` utilizes the CHAM membrane concept to model remotely distributed quantum systems. Each membrane is a self-contained computation node, representing a single-location quantum computation. It may contain many processes that can share quantum resources and perform intra-location communication, having concurrent behaviors. Membranes can also perform inter-membrane communication with each other, with some constraints imposed for capturing the quantum distributed system behaviors i.e., the communication between two different membranes can be either through a quantum channel, the abstraction of remote Bell pair used in quantum teleportation to transmit quantum qubit information, or classical message communications, such as the ones in π -calculus [Milner et al. 1992].

To properly identify quantum qubit resources in intra- and inter- communications, where qubits can be shared among processes and can only be communicated through quantum channels among membranes, we include the locus concept from `QAFNY` [Li et al. 2024], representing a group of qubits possibly being entangled, to allow users to locally identify the qubits in a membrane while keeping other unrelated qubits invisible to the membrane, as well as permit the sharing of qubits among processes in a single membrane. These properties are guaranteed by the `DisQ` type system.

To permit the equivalence between a sequential quantum program and its distributed version, we develop a new simulation relation based on the observation of quantum program measurement outputs. Instead of equating the step-by-step quantum operation behaviors, the `DisQ` simulation equates two quantum programs if their measurement results are the same with the same probability. To do so, we develop the `DisQ` semantics based on the Markov decision process (MDP), and transition labels are marked with probability values. This enables us to reason about the probability along a transition path towards a measurement outcome. However, this comes with some challenges – foremost among them stems from the fact that different branches of an MDP may result in the same measurement output. To address this challenge, we introduce the notion of simulation over a pair of sets of states rather than over a pair of individual states.

The major goal of `DisQ` is to help rewrite sequential quantum programs to distributed ones so that we can utilize NISQ computers to execute comprehensive quantum programs. The following enumerates the contributions of our work:

- We develop `DisQ`, with its syntax and semantics, to capture both single-location quantum concurrency and remote-location distributed quantum program behaviors, where we impose proper conditions on the system to allow users to explore the boundaries of distributing quantum algorithms.

- The language semantics is defined based on Markov decision processes [Puterman 1994], connecting quantum system behaviors with respect to probabilistic programming based on Markov decision processes.
- Based on the locus concept, we develop a type system where the type soundness guarantees the deadlock freedom in the system as well as the proper classification between single and remote location communications.
- Based on the MDP-based semantics, we develop a simulation relation to establish similarity (with respect to measurement) between sequential and distributed quantum programs.
- We conduct several representative case studies, including quantum addition circuits and Shor’s algorithm, and discuss the utility of DisQ in analyzing sequential quantum programs and their distributed versions. Specifically, the quantum teleportation case study shows that quantum entanglement can also be thought of as quantum information, capable of teleporting from one qubit to another.

2 BACKGROUND

Here, we provide background information on quantum computing, describing concurrent and distributed quantum systems. We show related works in Section 8.

Quantum Data. A quantum state (datum)¹ consists of one or more quantum bits (*qubits*), which can be expressed as a two-dimensional vector $\begin{pmatrix} \alpha \\ \beta \end{pmatrix}$ where the *amplitudes* α and β are complex numbers and $|\alpha|^2 + |\beta|^2 = 1$. We frequently write the qubit vector as $\alpha |0\rangle + \beta |1\rangle$ (the Dirac notation [Dirac 1939]), where $|0\rangle = \begin{pmatrix} 1 \\ 0 \end{pmatrix}$ and $|1\rangle = \begin{pmatrix} 0 \\ 1 \end{pmatrix}$ are *computational basis-kets*. When both α and β are non-zero, we can think of the qubit being “both 0 and 1 at once,” a.k.a. in a *superposition* [Nielsen and Chuang 2011], e.g., $\frac{1}{\sqrt{2}}(|0\rangle + |1\rangle)$ represents a superposition of $|0\rangle$ and $|1\rangle$. Larger quantum data can be formed by composing smaller ones with the *tensor product* (\otimes) from linear algebra. For example, the two-qubit datum $|0\rangle \otimes |1\rangle$ (also written as $|01\rangle$) corresponds to vector $[0\ 1\ 0\ 0]^T$. However, many multi-qubit data cannot be *separated* and expressed as the tensor product of smaller data; such inseparable quantum data are called *entangled*, e.g. $\frac{1}{\sqrt{2}}(|00\rangle + |11\rangle)$, known as a *Bell pair*. We can rewrite the Bell pair to $\sum_{b=0}^1 \frac{1}{\sqrt{2}} |bb\rangle$, where bb is a bit string consisting of two bits, each of which must be the same value (i.e., $b = 0$ or $b = 1$). Each term $\frac{1}{\sqrt{2}} |bb\rangle$ is named a *basis-ket* [Nielsen and Chuang 2011], consisting an amplitude ($\frac{1}{\sqrt{2}}$) and a basis $|bb\rangle$.

Quantum Computation and Measurement. Computation on a quantum datum consists of a series of *quantum operations*, each acting on a subset of qubits in the quantum datum. In the standard presentation, quantum computations are expressed as *circuits*, as shown in Figure 1, which depicts a circuit that prepares the Greenberger-Horne-Zeilinger (GHZ) state [Greenberger et al. 1989] — an n -qubit entangled datum of the form: $|\text{GHZ}^n\rangle = \frac{1}{\sqrt{2}}(|0\rangle^{\otimes n} + |1\rangle^{\otimes n})$, where $|d\rangle^{\otimes n} = \otimes_{j=0}^{n-1} |d\rangle$. In these circuits, each horizontal wire represents a qubit, and boxes on these wires indicate quantum operations, or *gates*. The circuit in Figure 1 uses n qubits and applies n gates: a *Hadamard* (H) gate and $n - 1$ *controlled-not* (CNOT) gates. Applying a gate to a quantum datum *evolves* it. Its traditional semantics is expressed by multiplying the datum’s vector form by the gate’s corresponding matrix representation: n -qubit gates are 2^n -by- 2^n matrices. Except for measurement gates, a gate’s matrix must be *unitary* and thus preserve appropriate invariants of quantum data’s amplitudes. A *measurement* (computational basis measurement)

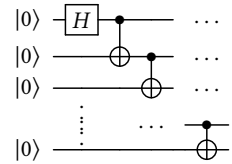


Fig. 1. GHZ Circuit

¹Most literature usually mentions quantum data as *quantum states*. In this paper, we refer to them as quantum data to avoid confusion between program and quantum states.

operation extracts classical information from a quantum datum. It collapses the datum to a basis state with a probability related to the datum's amplitudes (*measurement probability*), e.g., measuring $\frac{1}{\sqrt{2}}(|0\rangle + |1\rangle)$ collapses the datum to $|0\rangle$ with probability $\frac{1}{2}$, and likewise for $|1\rangle$, returning classical value 0 or 1, respectively. A more general form of quantum measurement is *partial measurement*, which measures a subset of qubits in a qubit array; such operations often have simultaneity effects due to entanglement, *i.e.*, in a Bell pair $\frac{1}{\sqrt{2}}(|00\rangle + |11\rangle)$, measuring one qubit guarantees the same outcome for the other – if the first bit is measured as 0, the second bit is too.

Quantum Concurrent, Networking, and Distributed Systems. Quantum networking techniques [Wehner et al. 2018] are developed for hybridizing the existing classical network infrastructure to construct the next generation of communication networks, a.k.a. quantum internet, featured with quantum mechanics [Granelli et al. 2022], which can provide more secure message communications than the existing infrastructure due to the *no-cloning* theorem, *i.e.*, quantum messages cannot be cloned, so hackers have no way to eavesdrop without being realized by users. Essentially, quantum networking techniques are based on quantum teleportation [Bennett et al. 1993; Rigolin 2005], where a Bell pair is viewed as quantum channels. Encoding messages in a party of a quantum channel leads to a change in the quantum state of the whole channel due to quantum entanglement. If the two parties of a quantum channel are located in different places, then the change in one party affects the other. The above teleportation circuit model serves as the theory basis while the real-world remote networking communication is based on more complicated networking techniques [Lago-Rivera et al. 2023; Pirandola et al. 2015; Shi and Qian 2020], different from the circuit-based quantum computing; such techniques have commercial usages [Earl et al. 2022] and researchers tried to develop SDN techniques for quantum communication [Buckley et al. 2024; Tessinari et al. 2023].

Quantum distributed computing utilizes quantum networking techniques to connect different single-location quantum computers to create a larger entanglement group, breaking the single-location computer entanglement scalability challenges [Padavic-Callaghan 2023], for executing comprehensive quantum algorithms in NISQ computers. The observation in many different quantum distributed computing studies and proposals [Barral et al. 2024; Caleffi et al. 2022; Cuomo et al. 2020; Davarzani et al. 2022; DiAdamo et al. 2021; Häner et al. 2021; Inc et al. 2024; Muralidharan 2024; Parekh et al. 2021; Tang and Martonosi 2024; Yimsiriwattana and Lomonaco Jr. 2004] is that there are always remote location entanglement links, supported by quantum teleportation, to connect different machines. The links are typically implemented as different kinds of techniques, other than single-location quantum circuits, because they want to keep each single-location quantum computer self-closed to ensure the coherence of single-location computers; such implementations can maximize the chance of creating large qubit entanglement groups across different quantum computers.

Quantum concurrent systems [Gheorghica 2023; Häner et al. 2022; Hillmich et al. 2020; Pysher et al. 2010] tried to utilize software and hardware multi-threaded techniques to improve the performance of executing quantum algorithms concurrently or parallelly. It is easy to confuse quantum concurrent and distributed systems. For example, [Meter and Devitt 2016] discussed how a quantum computer structure can be distributed to finish a task concurrently, and Beals et al. [2013] discussed how a single-location algorithm can be distributed to run in concurrent quantum systems. Because of the quantum decoherence limitations, single-location concurrent techniques might not achieve the goal of quantum distributed computing, so these two systems are different in the NISQ era.

Markov Chains and Decision Processes. A Markov chain [Markov 1906, 1907] is a stochastic model describing a sequence of possible events in which the probability of each event depends only

on the state attained in the previous event, and the probability of a program execution depends on the multiplication of the chain of the probabilities of events. It provides a standard labeled transition description of defining the semantic behaviors of probabilistic programming by viewing probabilistic as labels in semantic transitions; such labels are intrinsic and cannot be masked away. Markov decision process [Puterman 1994] extends a Markov chain by combining a nondeterministic choice with a probabilistic transition. Here, every step of computation is essentially a combination of two steps. We first make a nondeterministic choice—in DisQ, the choice is selecting membrane locations for an event happening—we then make a probabilistic move with a probability label.

3 OVERVIEW OF OUR SOLUTION STRATEGY

In this section, we present the features of our proposed language DisQ, discuss the rationale for these features, followed by the necessity (and challenges) for describing a new equivalence relation for proving the correctness of constructing distributed quantum programs as specified in DisQ with respect to its sequential version.

3.1 The CHAM Model and DisQ

The key ingredient of DisQ is its ability to model distributed quantum systems with explicit information about the remote location of the subsystems. This allows for specifying both intra-location (concurrent behaviors in a single location) and inter-location (distributed behaviors among remote locations) communication between subsystems. In light of this, the language is inspired largely by the *chemical abstract machine* (CHAM) description introduced by Berry and Boudol [Berry and Boudol 1992]. In the CHAM, the distributed and concurrent behavior of the system is modeled as chemical reactions between (abstract) molecules residing in a chemical solution that enables such reactions. The CHAM includes the concepts of *membranes* (or subsolutions), where the molecules inside the membranes can freely react; such behaviors correspond to concurrent behaviors. The reaction between molecules residing in two different membranes, corresponding to distributed behaviors, is allowed via a process referred to as *airlocking*. Intuitively, airlock allows for identifying and isolating a specific molecule in a membrane to get it ready for reaction with some other molecule (similarly airlocked) from a different membrane. The process allows for easily identifying the molecules that interact with each other in different membranes.

In DisQ, we use the concept of membranes to express the grouping of distributed subsystems in different locations; that is, each membrane can be viewed as a group of quantum systems at a particular location. We explicitly annotate the membranes with the location information to identify the locations of the quantum systems that are interacting with each other. Before formally presenting the language features of DisQ necessary for describing quantum systems, we provide a gentle introduction of the structure of DisQ with membranes, airlock, and standard process algebraic notion of concurrency (akin to π -calculus) to outline the salient features (and challenges) in developing DisQ.

Consider a simple grammar for communicating processes with membranes:

$$R ::= 0 \mid D.R \qquad D ::= a!v \mid a?(y) \qquad P ::= \{\bar{R}\}_l \mid R\{\bar{T}\}_l$$

In the above, a process of type R can be either a deadlocked process 0 or a sequential process where its behavior evolves by either performing a send-action ($a!v$: send v over channel a) or receive-action ($a?(y)$: receive some data over channel a and write to y). Two processes interact (synchronize) by sending and receiving messages over the same channel. The membrane description P is either a membrane $\{\bar{R}\}_l$ containing a multiset of processes of type R denoted by \bar{R} with explicit location information captured as l , or a membrane with an airlocked process $R\{\bar{T}\}_l$ where $R\{\bar{T}\}_l$ is ready to interact with some other airlocked process associated with a different membrane. A

program is a set of such membranes. Observe the inherent non-determinism in the interaction between processes within each membrane and between processes in different membranes. Any two processes in each membrane with appropriate send/receive actions may be non-deterministically selected for interaction; similarly, any two membranes with appropriate airlocked processes can be selected for interactions across membranes. This is similar to the CHAM model. We will augment the basic send/receive actions with actions involving the operations on quantum qubits and classical bits as necessary.

3.2 Markov Decision Processes and DisQ

In DisQ, to capture the probabilistic nature of the quantum systems, we introduce and associate probabilities with the semantics of each interaction. Unlike the CHAM model, where all interactions are nondeterministic, in our case, the choice of the membrane is nondeterministic, while the interaction proceeding the choice is probabilistic (e.g., the choice of the process that evolves in the non-deterministically selected membrane is probabilistic). Hence, in the presence of both nondeterminism and probabilities, the semantics of systems described in our language DisQ is captured using Markov Decision Processes (MDP), where each evolution involves a nondeterministic choice followed by a probabilistic move.

Consider the following example evolution of a system described in DisQ following the basic grammar described above:

$$\begin{aligned} \{\{a!v.0, 0\}_l, \{a?(y).0, 0\}_r\} &\xrightarrow{l.\frac{1}{2}} a!v.0\{0\}_l, \{a?(y).0, 0\}_r & (1) \\ &\xrightarrow{r.\frac{1}{2}} a!v.0\{0\}_l, a?(y).0\{0\}_r & (2) \\ &\xrightarrow{l.r.1} \{0, 0\}_l, \{0, 0\}_r & (3) \\ &\xrightarrow{l.1} \{0, 0\}_r \quad \xrightarrow{r.1} \emptyset & (4) \end{aligned}$$

There are two membranes at locations l and r , each containing two processes. Each step in the evolution includes a nondeterministic choice followed by a probabilistic one. For instance, in the first step (1), the nondeterministic choice results in the selection of membrane in location l (left membrane) followed by the probabilistic choice of airlocking the process $a!v.0$ in that membrane. This is presented in the annotation of the transition. Observe that, we have considered that selecting the processes in the left membrane is equally probable. Further, observe that there is another nondeterministic choice in selecting the membrane at location r . Proceeding further in the next step (2), we have considered a nondeterministic choice of selecting the membrane at location r followed by probabilistically selecting the process $a?(y).0$ to be airlocked. At this point, there are three nondeterministic choices: select the left membrane, select the right membrane, and select both membranes. The last choice is possible due to the presence of two airlocked processes in the membranes that are ready to interact. In Step (3), we show the third choice labeled as $l.r$ followed by the probability of interaction (in this case, the probability is 1 as there is exactly one probabilistic choice). In Step (3), we also implicitly present that the processes, after interacting, are absorbed back into their respective membranes.

Note that the multiplication of probabilities along a path shows the path probabilities, e.g., in the above example, the specific evolution happens with probability $\frac{1}{2} \times \frac{1}{2} \times 1 = \frac{1}{4}$. We permit the probabilistic selection of a terminating process (0), which can reflexively transition to itself, and a membrane can terminate, transitioning to \emptyset , only if all processes inside a membrane are 0, as in line (4).

3.3 Equivalence Relation for DisQ Programs

Given that DisQ program encodes distributed quantum programs, it is necessary to ensure the correctness of such encoding by comparing its behavior against the corresponding sequential quantum programs. Typically, the correctness is ensured by proving that any *relevant* behavior exhibited in the sequential program is also exhibited by its distributed counterpart, and vice versa. In process algebraic terms, such an equivalence is characterized using bisimulation, simulation, and trace equivalence relations. At a high level, these relations equate to the behavior of reachable configurations after one or more equivalent steps (see [Milner 1980] for details). Equivalence between steps is captured by the labels of the steps, and equivalence between configurations is decided by the valuations of variables that describe those configurations. In the context of distributed quantum programs (encoded by DisQ), such a notion of equivalence may not be appropriate.

First, the variables in the quantum programs involve both classical and quantum data. One of the key aspects of quantum data is that its impact is only manifested if measured. In other words, quantum states are not observable unless measured. Furthermore, the ordering of quantum operation on quantum data may not impact the result of its final measurement. For instance, applying an X gate followed by a Hadamard gate (H) on a qubit results in the same measure of the qubit when compared to the application of a H gate followed by a Z gate. Hence, the equivalence relation between configurations in a quantum program needs to be considered only in terms of the valuation of classical data and the measured quantum data; any quantum data that is not measured must not impact/decide the equivalence between the quantum configurations.

Second, the action labels in DisQ correspond to the location information capturing the nondeterministic choice and the probability associated with action for a process at the non-deterministically selected location. The specific location information, while important in describing programs in DisQ, is irrelevant for checking equivalence between two programs expressed in DisQ. A simple and straightforward way to address this issue is to discard the location information when describing the equivalence relation. This leaves us with the problem of handling the probability information that labels each transition/step. This problem can be intuitively described as follows. Consider that there is a system that evolves from a configuration G with probability 1 to a configuration G_1 and consider another system that evolves from a configuration H with probability p to a configuration H_1 and with probability $1 - p$ to a configuration H_2 , shown in Figure 2. Assume that the configurations G and H have the same relevant data and measurements, and similarly, configurations G_1 and each of H_1 and H_2 have the same data and measurements d . By the standard notions of (bi)simulation equivalence, G will not be equivalent to H owing to the fact the probability of evolution to G to G_1 does not "match" with the probability of evolution from H to H_1 or H to H_2 . However, the probability measure for G to evolve to G_1 , and H to H_1 and H_2 are identical (i.e., 1).

Therefore, it is necessary to introduce a new notion of equivalence relation. At its core, this new equivalence relation is defined over the set of equivalent configurations. When a configuration evolves, we partition the destination configurations into equivalent classes, and we compute the probability of evolving to each equivalent class as the sum of the probabilities leading to each element in the class. For instance, in the above abstract example, G evolves G_1 with probability 1. On the other hand, H evolves to H_1 and H_2 , where H_1 and H_2 are identical and hence belong to the same equivalent class. The probability for evolving from H to the class containing H_1 and H_2 is $p + (1 - p) = 1$. Based on this observation, we can conclude that G is equivalent to H because they are identical, and each can evolve to equivalent classes G_1 and $\{H_1, H_2\}$ with probability 1.

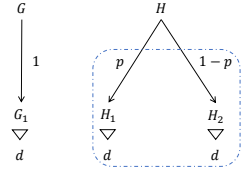


Fig. 2. Sim Diagram

Basic Terms:

| | | | | | | | |
|-----------|-----------------------|--------------|---|-----------|-------------|-----------------------|-----------|
| Nat. Num | $m, n \in \mathbb{N}$ | Bit | $b ::= 0 \mid 1$ | Bitstring | $d \in b^*$ | Variable/Classic Chan | x, y, a |
| Amplitude | $z \in \mathbb{C}$ | Basis Vector | $\beta ::= \langle d\rangle \rangle^*$ | Location | l, r, u | Quantum Chan | c |

Modes, Kinds, Types, and Classical/Quantum Data:

| | |
|-----------------------|---------------------------------------|
| Kind | $g ::= \mathbb{C} \mid \mathbb{Q}(n)$ |
| Classical Scalar Data | $v ::= d \mid n$ |
| Frozen Basis Stack | $\gamma ::= \langle \beta \rangle$ |
| Full Basis Vector | $\eta ::= \beta\gamma$ |
| Basic Ket | $w ::= z\eta$ |
| Quantum Type | $\tau ::= \text{EN} \mid \dots$ |
| Quantum Data | $q ::= \sum_{j=0}^m w_j$ |

Quantum Loci, Environment, and States

| | | | |
|----------------------------|---|-----------------|----------|
| Qubit Array Range | $s ::= x[n, m]$ | | |
| Local Locus | $\kappa ::= \bar{s}$ | concatenated op | \sqcup |
| Locus | $K ::= \overline{\langle \kappa \rangle}_l$ | concatenated op | \sqcup |
| Kind Environment | $\Omega ::= x \rightarrow g$ | | |
| Local Type Environment | $\sigma ::= \overline{\kappa : \tau}$ | concatenated op | \sqcup |
| Type Environment | $\Sigma ::= \overline{K : \tau}$ | concatenated op | \sqcup |
| Local Quantum State (Heap) | $\varphi ::= \overline{\kappa : \bar{q}}$ | concatenated op | \sqcup |
| Quantum State (Heap) | $\Phi ::= \overline{K : q}$ | concatenated op | \sqcup |

Syntax Abbreviations and Basis/Locus Equations

$$\begin{aligned}
1\gamma &\simeq \gamma & \sum_{j=0}^0 w_j &\simeq w_0 & \sum_{j=0}^m w_j &\simeq \sum_j w_j & z\beta(\langle \emptyset \rangle) &\simeq z\beta & z\beta(\langle \beta' \rangle) &\simeq z\beta\beta' \\
x[n, n] &\equiv \emptyset & \emptyset \sqcup \kappa &\equiv \kappa & |d_1\rangle |d_2\rangle &\equiv |d_1 d_2\rangle & \langle q \sqcup q' \rangle_l &\equiv \langle q \rangle_l \sqcup \langle q' \rangle_l & x[n, m] &\equiv x[n, j] \sqcup x[j, m] \text{ if } j \in [n, m]
\end{aligned}$$

Fig. 3. DisQ element syntax. Each range $x[n, m]$ in a locus represents the number range $[n, m]$ in physical qubit array x . Loci are finite lists, while type environments and states are finite sets. The operations after "concatenated op" refer to the concatenation operations for loci, type environments, and quantum program states. Term a is no more than a variable, but we refer to it specifically for classical channels in this paper.

We will elaborate and formalize this new notion of our equivalence relation in Section 6.

4 DISQ DESIGN PRINCIPLES: LOCUS, STATE, AND SYNTAX

We develop the syntactic constructs necessary to encode distributed quantum algorithms in DisQ. As is typical of any programming language, we will proceed with the description of the type, structure, and valuations of data followed by the program-state and flow constructs used in the DisQ language. A simple running example will be used to discuss the features and expressive power of the proposed language.

4.1 DisQ Data Elements and States

We present the necessary data elements (types and values) that represent the states in quantum algorithms. The syntax follows from our prior work [Li et al. 2024] with specific augmentation to allow for capturing the data and state information in a distributed environment.

There are two kinds of data: scalar (\mathbb{C}) and quantum ($\mathbb{Q}(n)$, representing n qubits). For simplicity, in a local membrane, we assume no aliasing in variable names and no overlapping between qubit arrays referred to by any two different variables; variables and locations are in distinct categories. The valuation of scalar kind data is either of type bitstrings (d) or natural numbers (n). On the other hand, quantum data valuations are represented using a varied Dirac notation $\sum_{j=0}^m z_j \beta_j \eta_j$, where m is the number of basis-kets in the quantum data. We *extend* the basis-ket structure, such that each basis-ket datum contains not only an amplitude z_j and a basis vector β_j , but also a frozen basis stack η_j , which stores basis vectors not directly involved in the current computation. The necessity for the frozen basis stack will be elaborated on later while describing the semantics of the language.

| | |
|----------------------|---|
| Unitary Expr | μ |
| Bool Expr | B |
| Local Action | $A ::= \kappa \leftarrow \mu \mid x \leftarrow \mathcal{M}(\kappa)$ |
| Communication Action | $D ::= a!v \mid a?(y)$ |
| Process | $R, T ::= 0 \mid D.R \mid A.R \mid \text{if } (B) R \text{ else } T$ |
| Membrane | $P, Q ::= \{\bar{R}\}_l \mid R\{\bar{T}\}_l \mid \nu x(n).P \mid \partial c(n).P$ |

Fig. 4. DisQ Syntax. We have the syntactic sugar: $\text{if } (B) \{R\}.T = \text{if } (B) R.T \text{ else } T$.

The type of this quantum data describes how the qubit vectors relate to each other, introduced in Li et al. [2024]. This paper considers the most general type EN (entanglement).

Next, we describe the "state" representation scheme in DisQ programs. We include a kind environment (Ω) to classify variables in a DisQ program as a certain kind, classical or quantum, and classical variable evaluation is substitution based in DisQ. Quantum data are conceptually stored as a heap (a quantum state $\Phi \triangleq \overline{K : q}$), which is partitioned into regions described as loci (K) in DisQ; each region contains possibly entangled qubits, with the guarantee that cross-locus qubits are not entangled. Each locus can be viewed as a chain of disjoint region segments labeled with explicit information about the location of local state variables, e.g., $\langle c[0] \rangle_l \sqcup \langle c[0] \rangle_r$ suggests that the two qubits, both named $c[0]$, in locations l and r are possibly entangled. Note that we have applied the membrane notation to capture this location-based information.

In describing a local quantum state (φ) for a location, we disregard the location information; thus, we can utilize local loci (κ) to refer to a quantum datum locally to a specific location. Each local locus consists a list of *disjoint ranges* (s), each represented by $x[n, m]$ —an in-place array slice selected from n to m (exclusive) in a physical qubit array x (always being Q kind). Ranges in a local locus are pairwise disjoint, written as $s_1 \sqcup s_2$. For conciseness, in our examples, we abbreviate a singleton range $x[j, j+1]$ as $x[j]$. The quantum type of these quantum data describes their relationship and is denoted by $\Sigma \triangleq \overline{K : \tau}$ associated with the corresponding valuations $\Phi \triangleq \overline{K : q}$. We also include local type environments $\sigma \triangleq \overline{\kappa : \tau}$ associated with the corresponding valuations $\varphi \triangleq \overline{\kappa : q}$, which forms the state at each location (referred to as a local state).

Figure 3 also presents some notational convenience and equivalences. The notation \simeq is used for abbreviations. For instance, we omit the frozen basis stack notation ($\{\bar{\cdot}\}$) in a basis-ket presentation and **color** the frozen basis stack with a hat sign $\hat{\cdot}$, e.g., $\frac{1}{\sqrt{2}} |0\rangle \{\hat{1}\}$ means $\frac{1}{\sqrt{2}} |0\rangle \{\bar{1}\}$; additionally, $\frac{1}{\sqrt{2}} |0\rangle \{\bar{1}\}$ means $\frac{1}{\sqrt{2}} |0\rangle \{\bar{1}\} \{\emptyset\}$.

4.2 Syntax for The DisQ Language

A DisQ encoding of a distributed quantum algorithm is described using a multiset of location-specific quantum processes. We define the syntax (Figure 4) over a membrane (a concept borrowed from the CHAM: see Section 3.1). There are three types of membrane descriptions: a multiset of processes ($\{\bar{R}\}_l$) with location information (l), an airlocked process associated with a membrane ($R\{\bar{T}\}_l$) and a membrane which evolves after a new length n channel ($\partial c(n)$) or qubit array ($\nu x(n)$) is initiated ($\nu x(n).P$ or $\partial c(n).P$). The last type is necessary to facilitate communication between processes in different membranes. The operation $\nu x(n)$ results in the generation of a blank array (x) of size n , and $\partial c(n)$ creates a quantum channel (c). If we have $\partial c(n).P, \partial c(n).Q$ with P and Q being in membranes l and r , they collaboratively create an $2n$ -qubit EPR pair, each membrane shares an n qubit array, pointed to by loci $\langle c[0, n] \rangle_l$ and $\langle c[0, n] \rangle_r$, respectively. This is similar to π -calculus style creation of new channels.

A process R , localized to a membrane, can be understood as a sequence of local (A) or communication actions (D). Here, we permit classical process algebraic message transmission operations

$$\begin{aligned}
(1) \quad & \{\emptyset\} \\
& \partial c(1). \{R\}_l. \partial c(1). \partial c'(1). \{c'[0] \sqcup c[0] \leftarrow CX.0, c'[0] \leftarrow X.0\}_u. \partial c'(1). \{T\}_r \\
(2) \quad & \xrightarrow{L.u.1} \{\langle c[0] \rangle_l \sqcup \langle c[0] \rangle_r : \sum_{j=0}^1 \frac{1}{\sqrt{2}} |jj\rangle\} \\
& \{R\}_l, \partial c'(1). \{c'[0] \sqcup c[0] \leftarrow CX.0, c'[0] \leftarrow X.0\}_u, \partial c'(1). \{T\}_r \\
(3) \quad & \xrightarrow{u.r.1} \{\langle c[0] \rangle_l \sqcup \langle c[0] \rangle_u : \sum_{j=0}^1 \frac{1}{\sqrt{2}} |jj\rangle \sqcup \langle c'[0] \rangle_u \sqcup \langle c'[0] \rangle_r : \sum_{m=0}^1 \frac{1}{\sqrt{2}} |mm\rangle\} \\
& \equiv \{\langle c[0] \rangle_l \sqcup \langle c[0] \sqcup c'[0] \rangle_u \sqcup \langle c'[0] \rangle_r : \sum_{j=0}^1 \sum_{m=0}^1 \frac{1}{2} |jjmm\rangle\} \\
& \{R\}_l, \{c'[0] \sqcup c[0] \leftarrow CX.0, c'[0] \leftarrow X.0\}_u, \{T\}_r \\
(4) \quad & \xrightarrow{u.\frac{1}{2}} \{\langle c[0] \rangle_l \sqcup \langle c'[0] \sqcup c[0] \rangle_u \sqcup \langle c'[0] \rangle_r : \sum_{j=0}^1 \sum_{m=0}^1 \frac{1}{2} |j(j \oplus m)jm\rangle\} \\
& \equiv \{\langle c[0] \rangle_l \sqcup \langle c'[0] \sqcup c[0] \rangle_u \sqcup \langle c'[0] \rangle_r : \frac{1}{2} (|0000\rangle + |0101\rangle + |1110\rangle + |1011\rangle)\} \\
& \{R\}_l, \{0, c'[0] \leftarrow X.0\}_u, \{T\}_r \\
(5) \quad & \xrightarrow{u.\frac{1}{2}} \{\langle c[0] \rangle_l \sqcup \langle c'[0] \sqcup c[0] \rangle_u \sqcup \langle c'[0] \rangle_r : \frac{1}{2} (|0100\rangle + |0001\rangle + |1010\rangle + |1111\rangle)\} \\
& \{R\}_l, \{0, 0\}_u, \{T\}_r
\end{aligned}$$

Fig. 5. The example of three membranes and two-channel creations. Transitioned DisQ programs are in black, and quantum states are in blue. Lines (3) and (4) contain different representations of the same state, equating by \equiv , described by *grayed out* states.

($a!v$ and $a?(y)$); they are the only communication actions that can perform direct message passing between different membranes, and the manipulations of quantum channels are done through local quantum actions that might lead to global side effects. We include quantum unitary operation $\kappa \leftarrow \mu$, applying a unitary operation μ to a local locus κ , as well as quantum measurement $x \leftarrow \mathcal{M}(\kappa)$, measuring the qubits referred to by κ and storing the result as a bitstring x . In DisQ, we abstract away the detailed implementation of μ and assume that they can be analyzed by some systems describing quantum unitary circuits, such as VOQC [Hietala et al. 2021b]. In a process, we also permit a classical conditional `if (B) R else T` with arguments (\bar{x}) being C kind. The expression B is arbitrary classical Boolean expression B , implemented using bit-arithmetic, i.e., 1 as true and 0 as false.

4.3 Running Example: How Locus Works

Here, we illustrate the evolution of a DisQ program with informal insights toward the semantics of the language. In subsequent sections, we will present the formal semantics of the language.

The program in Figure 5 line (1) describes a distributed system with three distinct membrane locations l , u , and r . In addition to the membrane information, we also present the state of the variables at each step of the program evolution; initially, this being $\{\emptyset\}$, i.e., no assignment to any variables has been decided. Line (2) collaboratively creates a quantum channel c across the two membranes l and u , by the two actions $\partial c(1)$ in the two membranes, indicating that these two membranes may be able to eventually exchange qubit information via the channel c . This collaboration between the l and u membranes is denoted by the evolution labeled with l and u (with probability measure 1) and results in the creation of a single qubit Bell pair; l and r both hold a qubit named $c[0]$, representing one end of the channel. This information is added to the data representation of the state resulting from the evolution. The quantum channel creation indicates a mechanism to identify the qubit scopes in different membranes, which is captured by the locus concept in DisQ.

Similarly, line (3) presents the construction of a quantum channel between membranes u and r . At this point, there are two equally probable choices for membrane u — $c'[0] \sqcup c[0] \leftarrow CX.0$ and $c'[0] \leftarrow X.0$. In either case, the processes are "action" prefixed, and the action involves local quantum actions that might affect the quantum channels shared with other membranes. Hence, the only possibility for each process in u is to perform the two local actions. In the example, for the

evolution to the line (4), we consider that the first process to make a move to apply a controlled-not gate (CX) to the local locus fragment $c'[0] \sqcup c[0]$ in membrane u , as illustrated by the evolution labeled with u with probability $1/2$. In line (3), the state shows that the local locus fragment is not in the same order, i.e., $c[0] \sqcup c'[0]$. To perform the application, we transform the locus from left to right, which simultaneously changes the locus's datum form in the associated state:

$$\langle c[0] \rangle_l \sqcup \langle c[0] \sqcup c'[0] \rangle_u \sqcup \langle c'[0] \rangle_r : \sum_{j=0}^1 \sum_{m=0}^1 \frac{1}{2} |j\rangle |j\rangle |m\rangle |m\rangle \quad \langle c[0] \rangle_l \sqcup \langle c'[0] \sqcup c[0] \rangle_u \sqcup \langle c'[0] \rangle_r : \sum_{j=0}^1 \sum_{m=0}^1 \frac{1}{2} |j\rangle |j\rangle |m\rangle |m\rangle$$

Here, each position in a locus corresponds to the qubit basis vector in the quantum state, i.e., the red arrows indicate the correspondence of the locus positions and its qubit basis vector. Rewriting locus structures automatically rewrite their corresponding basis vector structures, such as the rewrite from left to right above. We call the corresponding basis bits of qubits or locus fragments for a datum (or a basis-ket set) as the *qubit's/locus's position bases* of the datum (or the basis-ket set). Locus-type-state simultaneity permits the manipulation of a locus's position bases and data without observing the actual quantum state, e.g., to apply the CX gate, we manipulate the type environment associated with the quantum state to swap the order of $c[0]$ and $c'[0]$, so that the locus is in the correct form for the application. The type-guided rewrite rules are described in Li et al. [2024]. We describe some of them as equivalence rules in Figure 3, e.g., 1) the locus concatenation \sqcup holds identity and associativity equational properties; 2) a range $(x[n, n])$ containing 0 qubit is empty; and 3) we are free to split a range $(x[n, m])$ into two $(x[n, j])$ and $(x[j, m])$, which preserves the disjointness requirement for \sqcup . Further examples will be presented in Section 5.2.

Another use case of loci is to enable locality for inferring the local version of a locus by collecting all qubits only related to a specific membrane and by placing other qubits in *frozen basis stacks*. The following example illustrates the scenario.

Example 4.1 (One Step Application). e and e' are the line (5) in Figure 5 and $K \triangleq \langle c'[0] \sqcup c[0] \rangle_u \sqcup \langle c[0] \rangle_l \sqcup \langle c'[0] \rangle_r$.

$$\frac{(\langle c'[0] \sqcup c[0] \rangle : \sum_{j=0}^1 \sum_{m=0}^1 \frac{1}{2} |mj\rangle \overline{|jm\rangle}), c'[0] \sqcup c[0] \leftarrow \text{CX}.0) \xrightarrow{1} (\langle c'[0] \sqcup c[0] \rangle : \sum_{j=0}^1 \sum_{m=0}^1 \frac{1}{2} |(j \oplus m)j\rangle \overline{|jm\rangle}), 0)}{(\{K : \sum_{j=0}^1 \sum_{m=0}^1 \frac{1}{2} |mjjm\rangle\}, e) \xrightarrow{u.1} (\{K : \sum_{j=0}^1 \sum_{m=0}^1 \frac{1}{2} |(j \oplus m)jjm\rangle\}, e')}$$

In the above example, the CX gate application is local to membrane u , and we localize the quantum state to only mention the qubits in u , as the state rewrites from the bottom to the upper level. However, quantum states might involve entanglement, and the unreachable and entangled qubits must be indirectly mentioned to reflect the entanglement properties. We utilize the frozen stack in each basis-ket to record their states. For example, when we hide the locus fragment $\langle c[0] \rangle_l \sqcup \langle c[0] \rangle_r$ in the system, we push its position bases to the frozen stacks, which are the unreachable positions with respect to the local locus in u .

5 DISQ FORMALISM

This section presents the DisQ's semantics, the type systems, and the type soundness theorem.

5.1 DisQ Semantics

The DisQ semantics is based on a combination of Markov-chain and Markov-decision process and can be divided into two categories, for process and membrane level semantics. The process level

$$\begin{array}{c}
\text{S-SELF} \qquad \qquad \qquad \text{S-OP} \\
(\varphi, 0) \xrightarrow{1} (\varphi, 0) \qquad (\varphi \uplus \{\kappa \boxplus \kappa' : q\}, \kappa \leftarrow \mu.R) \xrightarrow{1} (\varphi \uplus \{\kappa \boxplus \kappa' : \llbracket \mu \rrbracket^{|\kappa|} q\}, R) \\
\\
\text{S-IFT} \qquad \qquad \qquad \text{S-IFF} \\
(\varphi, \text{if } (1) R \text{ else } T) \xrightarrow{1} (\varphi, R) \qquad (\varphi, \text{if } (0) R \text{ else } T) \xrightarrow{1} (\varphi, T) \\
\\
\text{S-MEA} \\
\frac{p = \sum_j |z_j|^2}{(\varphi \uplus \{\kappa \boxplus \kappa' : \sum_j z_j |d\rangle \eta_j + q \langle \kappa, d \neq \kappa \rangle\}, x \leftarrow \mathcal{M}(\kappa).R) \xrightarrow{d.p} (\varphi \uplus \{\kappa' : \sum_j \frac{z_j}{\sqrt{p}} \eta_j\}, R[d/x])} \\
\llbracket \mu \rrbracket^n (\sum_j z_j |d_j\rangle \eta_j) \triangleq \sum_j z_j (\llbracket \mu \rrbracket |d_j\rangle) \eta_j \quad \text{where } \forall j |d_j| = n \\
(\sum_i z_i |c_i\rangle \eta_i + q) \langle \kappa, b \rangle \triangleq \sum_i z_i |c_i\rangle \eta_i \quad \text{where } \forall i. |c_i| = |\kappa| \wedge \llbracket b[c_i/\kappa] \rrbracket = \text{true}
\end{array}$$

Fig. 6. DISQ single process semantic rules.

semantics is shown in Figure 6, which is expressed as a labeled transition system $(\varphi, R) \xrightarrow{\xi.p} (\varphi', T)$, where R and T are processes, φ and φ' are the pre- and post- local quantum states described in Figure 3, ξ is the transition label being empty (ϵ) or a measurement result v , and p is the probability of the single step transition. The membrane level semantics defines the nondeterministic behaviors of a DISQ program, shown in Figure 7. It is formalized as a labeled transition system $(\Phi, \bar{P}) \xrightarrow{\alpha.p} (\Phi', \bar{Q})$ where α (either $l.\xi$ or $l.r.\xi$) captures the membrane locations (l or $l.r$) participating in the nondeterministic choice of the transition followed by a possible measurement result (ξ), p represents the probability of the transition, and Φ and Φ' are the global pre- and post- quantum states described in Figure 3, mapping from global loci to quantum values.

Process Level Semantics. A DISQ process is a sequence of actions, and rules in Figure 6 define the semantics for a local action prefixed in a process. Rule S-SELF shows that the process semantics in a membrane is reflexive and can make a move to itself to preserve the stochastic property in a Markov chain, explained shortly below. Rule S-OP applies a quantum unitary operation to a locus κ state. Here, the locus fragment κ to which the operation is applied must be prefixed in the locus $\kappa \boxplus \kappa'$ that refers to the entire quantum state q . If not, we will first apply equivalence rewrites, explained in Section 5.2 and Li et al. [2024], to move κ to the front. With κ preceding the rest fragment κ' , the operation's semantic function $\llbracket \mu \rrbracket^n$ is then applied to κ 's position bases in the quantum value q . More specifically, the function is only applied to the first n (equal to $|\kappa|$) basis bits of each basis-ket in the value while leaving the rest unchanged. For example, in Figure 5 line (4), to apply X to the qubit $c'[0]$ in membrane u , not only do we need to perform the frozen qubit procedure in Example 4.1 to freeze qubits outside membrane u so we focus on a local locus to u , as $c'[0] \boxplus c[0]$, but also do we need to ensure that $c'[0]$ is prefixed in the local locus.

A measurement $(x \leftarrow \mathcal{M}(\kappa).R)$ collapses qubits in a locus κ , binds a C-kind integer to x , and restricts its usage in R . Rule S-MEA shows the partial measurement behavior². Assume that the locus is $\kappa \boxplus \kappa'$; the measurement is essentially a two-step array filter: (1) the basis-kets of the value is partitioned into two sets (separated by +): $(\sum_{j=0}^m z_j |d\rangle |d_j\rangle) + q \langle \kappa, d \neq \kappa \rangle$, by randomly picking a $|\kappa|$ -length basis d where every basis-ket in the first set have κ 's position basis d ; and (2) we create a new array value by removing all the basis-kets not having d as prefixes (the $q \langle \kappa, d \neq \kappa \rangle$ part) and also removing the κ 's position basis in every remaining basis-ket; thus, the quantum value becomes $\sum_{j=0}^m \frac{z_j}{\sqrt{p}} \eta_j$. Notice that the size $m+1$, the element size of the post-state, is smaller than the size of the pre-state before the measurement. Since the amplitudes of basis-kets must satisfy $\sum_i |z_i|^2 = 1$, we need to normalize the amplitude of each element in the post-state by multiplying a

²A complete measurement is a special case of a partial measurement when κ' is empty in S-MEA

$$\begin{array}{c}
\text{S-MEM} \\
\frac{n = |R, \bar{T}|}{(\Phi, \{D.R, \bar{T}\}_l) \xrightarrow{L, \frac{1}{n}} (\Phi, D.R\{\bar{T}\}_l)} \\
\\
\text{S-MOVE} \\
\frac{n = |R, \bar{T}| \quad (\{\kappa : S^{|\kappa|}(q)\}, R) \xrightarrow{\xi, p} (\{\kappa' : q'\}, R')}{(\Phi \uplus \{\langle \kappa \rangle_l \uplus K : q\}, \{R, \bar{T}\}_l) \xrightarrow{L, \xi, \frac{p}{n}} (\Phi \uplus \{\langle \kappa' \rangle_l \uplus K : F(q')\}, \{R', \bar{T}\}_l)} \\
\\
\text{S-COMM} \quad \text{S-NEWVAR} \\
\frac{(\Phi, a!v.R\{\bar{M}\}_l, a?(x).T\{\bar{N}\}_r) \xrightarrow{L, r, 1} (\Phi, \{R, \bar{M}\}_l, \{T[v/x], \bar{N}\}_r) \quad \text{loc}(P) = l}{(\Phi, vx(n).P) \xrightarrow{L, 1} (\Phi \uplus \{\langle x[0, n] \rangle_l \mapsto |\bar{0}\rangle\}, P)} \\
\\
\text{S-NEWCHAN} \\
\frac{\text{loc}(P) = l \quad \text{loc}(Q) = r}{(\Phi, \partial c(n).P, \partial c(n).Q) \xrightarrow{L, r, 1} (\Phi \uplus \{\langle c[0, n] \rangle_l \uplus \langle c[0, n] \rangle_r \mapsto \bigotimes_{j=0}^{n-1} (\sum_{d=0}^1 \frac{1}{\sqrt{2}} |\bar{d}\rangle)\}, P, Q)} \\
\\
\begin{array}{l}
S^n(\sum_j z_j |c_j\rangle \beta_j (|\beta'_j\rangle)) \triangleq \sum_j z_j \beta_j (|c_j\rangle \beta'_j) \quad \text{where } \forall j |c_j| = n \\
F(\sum_j z_j \beta_j (|c_j\rangle \beta'_j)) \triangleq \sum_j z_j |c_j\rangle \beta_j (|\beta'_j\rangle)
\end{array}
\end{array}$$

Fig. 7. Membrane-level semantic rules. $\text{loc}(P)$ produces the location in membrane P .

factor $\frac{1}{\sqrt{p}}$, with $r = \sum_{j=0}^m |z_j|^2$ as the sum of the amplitude squares appearing in the post-state. The rule's transition probability is labeled with $d.p$, referring to the measurement result and probability of having the result. In Example 7.1 of Section 7.1, the measurement step ($w \leftarrow \mathcal{M}(c[0])$) in line (5) transits the state to the one in line (6). Here, the $c[0]$ qubit in membrane l has locus fragment $\langle c[0] \rangle_l$, whose position bases are $|0\rangle$ and $|1\rangle$ in the state $\sum_{d=0}^1 \frac{1}{\sqrt{2}} z_0 |0\rangle |dd\rangle - \frac{1}{\sqrt{2}} z_1 |1\rangle |(-d)d\rangle$. We then randomly pick 1 as the measurement result in line (6), with the probability of the pick being $\frac{1}{2}$. We then replace occurrence of w with 1 in the process in membrane l , resulting in $a!1.a!1.0$. Rule S-IFT and S-IFF describe the semantics of classical conditionals.

Membrane Level Semantics. Figure 7 shows the membrane level semantics. A DisQ program is a set of membranes. We assume that the evaluation of the membrane set is compositional, i.e., every subset of the set can make a move.

The transitions of the processes in a membrane can be understood as a Markov chain, in the sense that every process in a membrane has the chance to be selected to perform a location action or a communication action that requires an airlock step. This indicates that the chance of selecting any of the processes in a membrane equals $\frac{1}{n}$, where n is the number of processes in the membrane. The connection between a process transition and a membrane level transition, with the above probability chance calculation, is encoded as rules S-MEM and S-MOVE. The former handles the airlock mechanism for airlocking a process, ready for communication with another membrane, and the latter connects local action transitions with transition behaviors at the membrane level.

In S-MOVE, the locus $\langle \kappa \rangle_l \uplus K$ is assumed to map to the value q in the quantum state, and the prefixed action in R coincidentally is applied to the locus κ (in membrane l), which is guaranteed by the DisQ type system. In evaluating one step action in R , we use the operator $S^{|\kappa|}$ to select the κ 's position bases and push the rest of the position bases to the frozen basis stacks. Once the process level transitions the state to $\kappa' : q'$, we pull back the frozen bases from the stacks through the operator F and manage the global final state for the global locus $\langle \kappa' \rangle_l \uplus K$ to be $F(q')$. In the label $L, \xi, \frac{p}{n}$, we make a nondeterministic choice of location l , p is the probability of a one-step move in R , and ξ is the label associated with the location action transitions introduced in Figure 6. Rule S-REV

$$\begin{array}{c}
\text{T-PAR} \\
\frac{\sigma \leq \sigma' \quad \Omega; \sigma' \vdash e \triangleright \sigma''}{\Omega; \sigma_1 \uplus \sigma \vdash e \triangleright \sigma_1 \uplus \sigma''} \\
\\
\text{T-PARM} \\
\frac{\Sigma \leq \Sigma' \quad \Omega; \Sigma' \vdash P \triangleright \Sigma''}{\Omega; \Sigma_1 \uplus \Sigma \vdash P \triangleright \Sigma_1 \uplus \Sigma''} \\
\\
\text{T-OP} \\
\frac{\Omega; \sigma \uplus \{\kappa \boxplus \kappa' : \tau\} \vdash R \triangleright \sigma'}{\Omega; \sigma \uplus \{\kappa \boxplus \kappa' : \tau\} \vdash \kappa \leftarrow \mu. R \triangleright \sigma'} \\
\\
\text{T-MEA} \\
\frac{\Omega; \sigma \uplus \{\kappa' : \tau\} \vdash R \triangleright \sigma'}{\Omega; \sigma \uplus \{\kappa \boxplus \kappa' : \tau\} \vdash x \leftarrow \mathcal{M}(\kappa). R \triangleright \sigma'} \\
\\
\text{T-IF} \\
\frac{\Omega \vdash B : C \quad \Omega; \sigma \vdash R \triangleright \sigma' \quad \Omega; \varphi \vdash T \triangleright \sigma'}{\Omega; \sigma \vdash \text{if } (B) R \text{ else } T \triangleright \sigma'} \\
\\
\text{T-SEND} \\
\frac{\Omega \vdash a : C \quad \Omega \vdash v : C \quad \Omega; \sigma \vdash R \triangleright \sigma'}{\Omega; \sigma \vdash a!v. R \triangleright \sigma'} \\
\\
\text{T-REV} \\
\frac{\Omega \vdash a : C \quad \Omega[x \mapsto C]; \sigma \vdash R \triangleright \sigma'}{\Omega; \sigma \vdash a?(x). R \triangleright \sigma'} \\
\\
\text{T-NEW} \\
\frac{\text{loc}(P) = l \quad \Omega[x \mapsto Q(n)]; \Sigma \uplus \{\langle c[0, n] \rangle\}_l : \text{EN} \vdash P \triangleright \Sigma'}{\Omega; \Sigma \vdash \nu x(n). P \triangleright \Sigma'} \\
\\
\text{T-NEWC} \\
\frac{\text{loc}(P) = l \quad \Omega[c \mapsto Q(n)]; \Sigma \uplus \{\langle c[0, n] \rangle\}_l : \text{EN} \vdash P \triangleright \Sigma'}{\Omega; \Sigma \vdash \partial c(n). P \triangleright \Sigma'} \\
\\
\text{T-TOP} \\
\frac{\text{loc}(P) = l \quad \Omega; \langle \sigma \rangle_l \vdash P \triangleright \langle \sigma' \rangle_l \quad \Omega; \Sigma \vdash \bar{Q} \triangleright \Sigma'}{\Omega; \langle \sigma \rangle_l \uplus \Sigma \vdash P, \bar{Q} \triangleright \langle \sigma' \rangle_l \uplus \Sigma'} \\
\\
\text{T-MEM} \\
\frac{\text{has_mea}(\bar{R}) \quad \neg \text{has_mea}(\bar{T}) \quad \forall j \in [0, |\bar{R}|]. \Omega; \sigma_j \vdash \bar{R}_j \triangleright \sigma'_j \quad \Omega; \sigma \vdash \bar{T} \triangleright \sigma'}{\Omega; \langle \bigoplus_{j \in [0, |\bar{R}|]} \sigma_j \uplus \sigma \rangle_l \vdash \{\bar{R}, \bar{T}\}_l \triangleright \langle \bigoplus_{j \in [0, |\bar{R}|]} \sigma'_j \uplus \sigma' \rangle_l} \\
\langle \sigma \rangle_l \triangleq \forall \langle \kappa \rangle_r : \tau \in \langle \sigma \rangle_l. r = l
\end{array}$$

Fig. 8. DisQ type system. $\text{has_mea}(\bar{R})$ means every $R \in \bar{R}$ contains a measurement operation syntactically.

permits the release of an airlock. Section 7.1 shows example transitions with nondeterministic choices and airlocks.

Note that, in DisQ, every membrane has a fixed amount of processes in its lifetime. In rules S-MEM and S-MOVE, each probabilistic choice of performing a process has a probability $\frac{1}{n}$ where n is the number of processes in the membrane. To guarantee the equal distribution of the probabilistic choice of a process, we include rule S-SELF in Figure 6, as a 0 process can make a move to itself. One example execution is the possible transition branching in Figure 5 line (4). Here, the 0 process in membrane u is eligible for the process selection that produces a probability label $\frac{1}{2}$. In the end, if every process in a membrane turns to 0, rule S-END permits the termination of the membrane.

Rule S-NEWVAR introduces a new blank n -qubit quantum array in the membrane l . Rule S-NEWCHAN creates a new quantum channel between the membranes l and r , which results in a $2n$ -qubit Bell pair connecting l and r , each of which shares n qubits, referred to by the channel name c . The DisQ type system ensures that the two different c arrays are only used in the two different membranes, respectively; thus, no name collision is introduced. Rule S-COMM performs a classical message communication inherited from traditional π -calculus [Milner et al. 1992].

Both S-NEWCHAN and S-COMM transitions have labels $l.r.1$, meaning that the nondeterministic event happens across the l and r membranes. The probability 1 in the above three rules indicates that the transitions happen 100% once a nondeterministic choice is made.

5.2 DisQ Type System

Similar to DisQ semantics, the DisQ type system also has two levels of typing judgments. The membrane level judgment is $\Omega; \Sigma \vdash \bar{P} \triangleright \Sigma'$, stating that \bar{P} is well-typed under the environments Ω and Σ . The process level typing judgment is $\Omega; \sigma \vdash \bar{R} \triangleright \sigma'$, stating that \bar{R} is well-typed under the environments Ω and σ . The C-mode variables in a kind environment Ω are populated through message receipt and quantum measurement operations, while the Q-kind variables are populated through a quantum qubit $\nu x(n)$ or channel $\partial c(n)$ creation operation. The type rules are in Figure 8. For every type rule, well-formed domains ($\Omega \vdash \text{dom}(\Sigma)$) (or ($\Omega \vdash \text{dom}(\sigma)$)) are required but hidden

from the rules, such that every variable used in all loci of Σ (or σ) must appear in Ω . The type system enforces three properties below.

Ensuring Proper Parameter Kinds and Scopes. The type system ensures the scoping properties in variables and channels, e.g., quantum channels and variables have kind $Q(n)$, while classical channels and variables have kind C . Quantum variables and channels can possibly be modified inside a membrane but cannot be referred to by operations from distinct membranes, and some operations, such as message sending and receiving, can only refer to classical variables and channels. All these scoping properties are enforced by the type system. The Boolean ($\Omega \vdash B : C$) and arithmetic ($\Omega \vdash v : C$) expression checks (Appendix A) in rules T-IF, T-SEND, and T-REV, ensure that these expressions can only produce classical results and that their parameters are classical. Rule T-NEW ensures that all the quantum parameters mentioned in a membrane are properly initialized. Here, $\text{loc}(P)$ produces the location information about P , which is used to ensure that the newly generated locus $\langle x[0, n] \rangle_l$ (or $\langle c[0, n] \rangle_l$) mentions the right location.

Ensuring Proper Locus Partitioning. The type system also ensures that loci are properly partitioned in different membranes, and each membrane refers only to the permitted local loci. Rule T-TOP ensures a properly separated analysis of different loci and quantum parameters in different membranes, where the structure $\langle \sigma \rangle_l$ is a subset of the type environment and represents a procedure of collecting all the loci referred to membrane P residing in location l , and type check P with the subset $\langle \sigma \rangle_l$. As an instant in Figure 5, the initialization of a quantum channel referred to by the locus $\langle c[0] \rangle_l \sqcup \langle c[0] \rangle_u$ happens in membranes l and u . In type checking, we enable the individual analysis of the two membranes. In analyzing membrane l , the type environment contains an element $\langle c[0] \rangle_l : \text{EN}$, and we refer $c[0]$ to locus $\langle c[0] \rangle_l$, while in analyzing membrane u , we refer $c[0]$ to locus $\langle c[0] \rangle_u$ in the environment. We explain more details of $\langle \sigma \rangle_l$ below.

Rule T-MEM connects the typing relation between a membrane and its processes by turning a membrane-level type environment, mapping from loci to types, to a process-level type environment mapping from local loci to types. Depending on whether or not a process contains measurement operations (has_mea), the quantum qubit resource sharing scheme is different. For a membrane having two groups of processes: \bar{R} , each of which contains a measurement operation, and \bar{T} , containing no measurements, we partition the type environment into σ and σ_j for $j \in [0, |\bar{R}|)$, separated by disjoint unions \sqcup . For R_j in \bar{R} , we type check the process with the local type environment σ_j , and we type check every process in \bar{T} with σ , since every process in \bar{T} can share the qubits mentioned in σ . The type-checking results are merged back to a global type environment with each local locus labeled with l , as $\langle \sqcup_{j \in [0, |\bar{R}|)} \sigma'_j \sqcup \sigma' \rangle_l$.

Guiding Locus Equivalence and Rewriting. The DisQ type system maintains the simultaneity of loci in type environments and quantum states through the type-guided state rewrites, formalized as equivalence relations. In DisQ, a locus represents a possibly entangled qubit group. In many applications, [Ambainis 2004; Beauregard 2003; Childs et al. 2007; Häner et al. 2017; Magniez et al. 2005; Nielsen and Chuang 2011; Rigolin 2005; Shor 1994], algorithms are usually constructed by a loop to add an additional qubit to an existing entanglement group at a time. In this case, we need to utilize the locus information in the type environment to guide the equivalence rewrites of states guarded by the locus. We associate a state φ , with a type environment σ by sharing the same domain, i.e., $\text{dom}(\varphi) = \text{dom}(\sigma)$. Thus, the environment rewrites (\leq) happening in σ gear the state rewrites (\equiv) in φ . One example rewrite is to add an additional qubit $x[j+1]$ to a local locus $x[0, j]$, and rewrite it to $\kappa(x[j-1] \sqcup x[0, j-1] \sqcup x[j])$, which can also cause the state rewrites happen accordingly as (from left to right):

$$\begin{aligned} \{x[0, j] : \text{EN}\} \quad \cup \{x[j] : \text{EN}\} &\leq \{x[0, j+1] : \text{EN}\} &\leq \{\kappa : \text{EN}\} \\ \{x[0, j] : \Sigma_{d=0}^1 \frac{1}{\sqrt{2}} |\bar{d}\rangle |1\rangle\} \cup \{x[j] : |0\rangle\} &\equiv \{x[0, j+1] : \Sigma_{d=0}^1 \frac{1}{\sqrt{2}} |\bar{d}\rangle |1\rangle |0\rangle\} &\equiv \{\kappa : \Sigma_{d=0}^1 \frac{1}{\sqrt{2}} |1\rangle |\bar{d}\rangle |0\rangle\} \end{aligned}$$

The details of type equivalence relations and their simultaneity with respect to state rewrites are introduced in Li et al. [2024] and Appendix B. The gearing is also useful in performing qubit position permutations, such as fulfilling the prefix requirement in unitary operations. In our type system, we provide T-PAR and T-PARM to perform equivalence rewrites as typing relationships in the process and membrane levels, respectively.

One of the key utilities of the equivalence relation is to enable the separated analyses of locus structures localized to specific membranes, as shown in the T-Top rule. In permitting such analyses, the one-directional equivalence rewrite is enough. For example, the quantum channel creation in Figure 5, creates an entangled locus $\langle c[0] \rangle_l \sqcup \langle c[0] \rangle_u$ in two different membranes. When we type check the program, we only need to utilize the entries $\langle c[0] \rangle_l : \text{EN}$ and $\langle c[0] \rangle_u : \text{EN}$ to analyze membrane l and u , respectively, because in a membrane, one can never refer to a locus in a different membrane. In analyzing membrane l above, we focus on the local locus only, related to l , such as $\langle c[0] \rangle_l$, with the recognition that other membranes might contain qubits that are entangled with $\langle c[0] \rangle_l$. When relating the typing with the semantics, we utilize T-PARM to show the following rewrite can happen:

$$\langle c[0] \rangle_l : \text{EN} \sqcup \langle c[0] \rangle_u : \text{EN} \leq \langle c[0] \rangle_l \sqcup \langle c[0] \rangle_u : \text{EN}$$

The above procedure shows how $\langle \sigma \rangle_l$ is computed in rule T-Top. When typing a quantum channel creation, we assume that each of the creation operations separately creates a qubit array localized to a membrane l , using the entry $\langle c[0] \rangle_l : \text{EN}$ to analyze processes in l . When showing the type preservation relation between the typing and the semantics, we use the equivalence rewrites to connect different loci that might entangled with each other, such as $\langle c[0] \rangle_l$ and $\langle c[0] \rangle_u$.

The DisQ Metatheory. We prove our type system's soundness with respect to the semantics, assuming well-formedness. The type soundness theorem is split into type progress and preservation. The theorems rely on the definitions of wellformed domains $(\Omega \vdash \Sigma)$ and wellformed states $(\Omega; \Sigma \vdash \Phi)$, shown in Appendix C. The progress theorem shows that there is no possibility for a DISQ configuration to have a deadlock, even though DISQ is a multi-threaded system. Certainly, a DISQ configuration can diverge, leading to future studies.

THEOREM 5.1 (DISQ TYPE PROGRESS). If $\Omega \vdash \Sigma$, and $\Omega; \Sigma \vdash \Phi$, there exists α, Σ' and \bar{P}' , $(\Phi, \bar{P}) \xrightarrow{\alpha} (\Phi', \bar{P}')$.

The type preservation shows that our type system ensures the three properties above and that the "in-place" style DISQ semantics can describe all different quantum operations without losing generality because we can always use the equivalence rewrites to rewrite the locus state in ideal forms.

THEOREM 5.2 (DISQ TYPE PRESERVATION). If $\Omega \vdash \Sigma$, $\Omega; \Sigma \vdash \bar{P} \triangleright \Sigma'$, $(\Phi, \bar{P}) \xrightarrow{\alpha} (\Phi', \bar{P}')$, and $\Omega; \Sigma \vdash \Phi$, then there exists Ω_1 and Σ_1 , $\Omega_1; \Sigma_1 \vdash \bar{P}' \triangleright \Sigma'$.

6 DISQ OBSERVABLE SIMULATION

Here, we provide a formal definition of the DISQ simulation, where we are interested in universal path properties, e.g., for all computation paths, the probability of a specific measure result is p ; such properties enable the construction of equivalence between a quantum program and its distributed version.

To utilize DISQ to rewrite a sequential quantum program to a distributed one, it is necessary to develop an equivalence checker to show the two programs are semantically equivalent; such a task

is typically tackled through (bi)simulation, i.e., two programs are equivalent, if and only if they are (bi)similar. As we mentioned in Section 3.3, the traditional (bi)simulation might be too strong to show the equivalence between a sequential and a distributed program. Here, we define the DisQ observable simulation relation based on the observable measurement results, the core component of the DisQ equivalence checker; example utilities are in Section 7.

The DisQ semantics (Section 5) describe a labeled transition system $(\Phi, \bar{P}) \xrightarrow{\alpha.p} (\Phi', \bar{P}')$, where Φ and Φ' are quantum states, \bar{P} and \bar{P}' are DisQ programs, and $\alpha.p$ is a label; α is either a label in the DisQ semantics ($l.\xi$ or $l.r.\xi$), or an invisible label (ϵ). We can view a pair (Φ, \bar{P}) of quantum state and DisQ program as a transition configuration. The DisQ observable simulation is defined over finite sets of configurations, named as G or H , each element in the set has the form $(\Phi, \bar{P})^p$, where (Φ, \bar{P}) is a transition configuration and the probability p is the accumulated probability. We define a syntactic sugar G^p (or H^t), where the extra flag p (or t) refers to that for all $(\Phi_j, \bar{P}_j)^{p_j}$, $p = \sum_j p_j$ (or $t = \sum_j p_j$), with $j \in [0, |M|)$. We also allow users to define label mask functions $\psi: \alpha \rightarrow \alpha$ to mask a specific set of labels to be invisible, i.e., users are allowed to perform $\psi(\alpha.p) = \alpha.p$ or $\psi(\alpha.p) = \delta.p$, where $\delta = \xi$ or $\delta = \epsilon$. We first define set transitions related set of transition configurations G below.

Definition 6.1 (DisQ Configuration Set Transition). Given a transition configuration set G , we define set transition $G \xrightarrow{\alpha} G_1^t$ below.

- for every $(\Phi_j, \bar{P}_j)^{p_j}$ in G , we have $(\Phi_j, \bar{P}_j) \xrightarrow{\alpha.t_j} (\Phi'_j, \bar{P}'_j)$, and G_1 contains all configurations $(\Phi'_j, \bar{P}'_j)^{p_j * t_j}$ transitioned from (Φ_j, \bar{P}_j) , and $t = \sum_j p_j * t_j$, with $j \in [0, |G|)$.

We can now define the DisQ observable simulation, where $\text{set}(G, t)$ is a predicate, defined as for all $(\Phi_j, \bar{P}_j)^{p_j} \in G$, $(\Phi_j, \bar{P}_j)^t \in \text{set}(G, t)$.

Definition 6.2 (DisQ Observable Simulation). Given two transition configuration sets G and H , G simulates H , written as $G \sqsubseteq H$, iff

- $G \xrightarrow{\alpha} G_1^p$, where $\alpha \neq \epsilon$, if there is H_1 , such that $H \xrightarrow{\alpha} H_1^t$, and $p \approx t$, and $\text{set}(G_1, 1) \sqsubseteq \text{set}(H_1, 1)$.
- $(\Phi, \bar{P}) \xrightarrow{\epsilon.p'} (\Phi', \bar{P}')$ with $(\Phi, \bar{P})^p \in G$, then $(G - \{(\Phi, \bar{P})^p\}) \cup \{(\Phi', \bar{P}')^{p * p'}\} \sqsubseteq H$.
- $(\Phi, \bar{Q}) \xrightarrow{\epsilon.t'} (\Phi', \bar{Q}')$ with $(\Phi, \bar{Q})^t \in H$, then $G \sqsubseteq (H - \{(\Phi, \bar{P})^t\}) \cup \{(\Phi', \bar{P}')^{t * t'}\}$.

One can develop a (on-the-fly) algorithm for observable simulation as a least fixed point computation of negation of simulation relation [Basu et al. 2001]. Instead of computing $G \sqsubseteq H$, we compute $\text{not_sim}(\{G\}, \{H\}) \triangleq \neg(G \sqsubseteq H)$. Here, we start with two configuration sets, each containing only the initial configurations, i.e., \bar{G} and \bar{H} are respectively initialized as $\{G\}$ and $\{H\}$, as they contain all the possible initial states for the two programs being simulated. In each iteration, we partition a configuration set in the different sets, if the transition configuration set leads to different labels, e.g., in the first iteration, we partition \bar{G} into different sets, such as $G = G_1 \uplus G_2 \uplus \dots$, for each G_j , we guarantee that $G_j \xrightarrow{\alpha_j} G_j^p$ for one observable label α_j . Then, we check if there is also a partition in H , such that $H = H_1 \uplus H_2 \uplus \dots$, for each H_j , we make sure that $H_j \xrightarrow{\alpha'_j} N_j^u$ for the same label α'_j . For G_j , if we cannot find H_j , such that $G_j \sqsubseteq H_j$, the not_sim predicate holds. Otherwise, we loops to check $\text{not_sim}(\{G_j\}, \{H_j\})$. We take the least-fixed point of the computation, and the negation of the computation result conducts the simulation relation between G and H .

We implement a DisQ interpreter in Java and implement the not_sim function on top of our DisQ interpreter as our simulation checker. We then utilize the simulation checker to validate the simulation relation between sequential quantum programs P and their distributed versions \bar{P}' , i.e.,

$\overline{P'} \sqsubseteq P$. Since P is typically a sequential program, a simulation check is enough to equate the two. Certainly, one can easily construct a bisimulation checker based on our simulation framework for other utilities. We enable the simulation checks for all case studies in the paper.

7 CASE STUDIES

Here, we show three examples of utilizing distributed systems to develop quantum distributed algorithms.

7.1 Quantum Teleportation For Ensuring Entanglement Information

Quantum teleportation is a quantum network protocol that teleports information about a qubit to remote locations. A key observation is that quantum entanglement is also a piece of information; thus, when teleporting a qubit, the possible entanglement associated with the qubit should also be kept by remote qubits.

To demonstrate the case, we use the program in Example 7.1 to teleport a qubit $x[1]$ – currently entangles with $x[0]$ – from membrane l to r . The program first creates a shared quantum channel between the two membranes, referred to by $\langle c[0] \rangle_l$ and $\langle c[0] \rangle_r$, and then teleports $x[1]$ to membrane r to store the information in $\langle c[0] \rangle_r$. The result should show that the entanglement between $x[0]$ and $x[1]$ is transferred to be an entanglement between $x[0]$ and $\langle c[0] \rangle_r$.

Example 7.1 (Quantum Teleportation Entanglement Preservation). The example has two membranes. The program code of membrane l is: $\partial c(1) . \{x[1] \sqcup c[0] \leftarrow CX . x[1] \leftarrow H . R\}_l$, and The program code of membrane r is: $\partial c(1) . \{T\}_r$. R and T are given as follows:

$$\begin{aligned} R &= u \leftarrow \mathcal{M}(x[1]) . w \leftarrow \mathcal{M}(c[0]) . a!u . a!w . 0 \\ T &= a?(u) . a?(w) . \text{if } (u) \{c[0] \leftarrow Z\} . \text{if } (w) \{c[0] \leftarrow X\} . 0 \end{aligned}$$

Membrane l has initially two qubit entangled state $x[0, 2] : z_0 |00\rangle + z_1 |11\rangle$. K_c and K_e are:

$$K_c = \langle c[0] \rangle_l \sqcup \langle c[0] \rangle_r \quad K_e = \langle x[0, 2] \sqcup c[0] \rangle_l \sqcup \langle c[0] \rangle_r$$

The following provides the first few transition steps, where $\neg b$ is the bit-flip of the bit b .

- (1) $(\{ \langle x[0, 2] \rangle_l : \sum_{b=0}^1 z_b |bb\rangle \}, \partial c(1) . \{x[1] \sqcup c[0] \leftarrow CX . x[1] \leftarrow H . R\}_l, \partial c(1) . \{T\}_r)$
- (2) $\xrightarrow{l.r.1} (\{ \langle x[0, 2] \rangle_l : \sum_{b=0}^1 z_b |bb\rangle, K_c : \frac{1}{\sqrt{2}} \sum_{b=0}^1 |bb\rangle \}, \{x[1] \sqcup c[0] \leftarrow CX . x[1] \leftarrow H . R\}_l, \{T\}_r)$
- (3) $\xrightarrow{l.1} (\{K_e : \sum_{b=0}^1 \frac{1}{\sqrt{2}} z_0 |00\rangle |bb\rangle + \frac{1}{\sqrt{2}} z_1 |11\rangle |(-b)b\rangle\}, \{x[1] \leftarrow H . R\}_l, \{T\}_r)$
- (4) $\xrightarrow{l.1} (\{K_e : \sum_{b=0}^1 \frac{1}{2} z_0 |0\rangle |0\rangle |bb\rangle + \frac{1}{2} z_0 |0\rangle |1\rangle |bb\rangle + \frac{1}{2} z_1 |1\rangle |0\rangle |(-b)b\rangle - \frac{1}{2} z_1 |1\rangle |1\rangle |(-b)b\rangle\}, \{R\}_l, \{T\}_r)$

In the above example, the system chooses to let membrane l proceed and perform two transition steps, by applying a CX and H gate operations to the loci $x[1] \sqcup c[0]$ and $x[1]$, and the transitions result in a quantum state at the line (4). Except for the first label, $l.r.1$, all other labels show a choice of l , referring to the nondeterministic choice of picking membrane l in the transition. The probabilities are labeled 1 in all these l choices since there is only one process choice in the membrane. Certainly, membrane choice is nondeterministic, and one can make the wrong choice, e.g., in line (3), instead of choosing membrane l to make a move, membrane r can perform the move. Its prefixed action is waiting for a message that is unavailable. In such a case, membrane r can wait for membrane l to perform a move, or it can perform rule S-REV to reverse the process and release the airlock.

After the transitions, process R in membrane l performs two measurements on the qubits $x[1]$ and $\langle c[0] \rangle_l$. The measurements have four possibilities, referring to the four possible ways of combining the two outcome bits for the two qubits. The final outcome of the four possibilities is the same. Below, we show the transitions of one of the possibilities by probabilistically choosing the measurement outputs of the two qubits to be 1. Here, $K'_e = \langle x[0] \sqcup c[0] \rangle_l \sqcup \langle c[0] \rangle_r$.

$$(5) \xrightarrow{L.1.\frac{1}{2}} (\{K'_e : \sum_{b=0}^1 \frac{1}{\sqrt{2}} z_0 |0\rangle |bb\rangle - \frac{1}{\sqrt{2}} z_1 |1\rangle |(-b)b\rangle\}, \{\mathbf{w} \leftarrow \mathcal{M}(c[0]).a!1.a!w.0\}_l, \{T\}_r)$$

$$(6) \xrightarrow{L.1.\frac{1}{2}} (\{\langle x[0] \rangle_l \boxplus \langle c[0] \rangle_r : z_0 |0\rangle |1\rangle - z_1 |1\rangle |0\rangle\}, \{a!1.a!1.0\}_l, \{T\}_r)$$

The above shows the transitions for the two measurement operations in membrane l . Line (5) performs the first measurement. As the process R in Example 7.1 measures $x[1]$ and assigns the bit value to u , which is 1 here. After the transition, every u occurrence is replaced by 1 in the process. The probability of the measurement is $\frac{1}{2}$, which is computed by a geometric sum of all the basis-kets $(\frac{1}{\sqrt{2}} z_0 |0\rangle |1\rangle |bb\rangle$ and $-\frac{1}{\sqrt{2}} z_1 |1\rangle |1\rangle |(-b)b\rangle$ for $b = 0$ or $b = 1$) where $x[1]$'s position basis is $|1\rangle$. Line (6) repeats the process of lines (5), but for measuring $\langle c[0] \rangle_l$ and assigning w to 1. In this procedure, $\langle c[0] \rangle_l$'s position basis is $|b\rangle$ for the basis-kets $\frac{1}{\sqrt{2}} z_0 |0\rangle |bb\rangle$ and $|(-b)\rangle$ for the basis-kets $-\frac{1}{\sqrt{2}} z_1 |1\rangle |(-b)b\rangle$, with $b = 0$ or $b = 1$. Measuring out 1 means that we left with $z_0 |0\rangle |1\rangle$ for the first group by setting b to 1, and $-z_1 |1\rangle |0\rangle$ for the second group by setting $-b$ to 1; the combination of the two basis-kets is the resulting state at line (6). In the procedure, the multiplication of the probabilities along the path of the transitions results in $\frac{1}{4}$, complying with the probability of measuring out two 1s for the $x[1]$ and $\langle c[0] \rangle_l$.

$$(7) \xrightarrow{L.1} (\{\langle x[0] \rangle_l \boxplus \langle c[0] \rangle_r : z_0 |0\rangle |1\rangle - z_1 |1\rangle |0\rangle\}, (a!1.a!1.0) \{\emptyset\}_l, \{T\}_r)$$

$$(8) \xrightarrow{r.1} (\{\langle x[0] \rangle_l \boxplus \langle c[0] \rangle_r : z_0 |0\rangle |1\rangle - z_1 |1\rangle |0\rangle\}, (a!1.a!1.0) \{\emptyset\}_l, T\{\emptyset\}_r)$$

...

$$(9) \xrightarrow{L.r.1} (\{\langle x[0] \rangle_l \boxplus \langle c[0] \rangle_r : z_0 |0\rangle |1\rangle - z_1 |1\rangle |0\rangle\}, \{a!1.0\}_l, \{a?(w).c[0] \leftarrow Z.\text{if}(w)\{c[0] \leftarrow X\}.0\}_r)$$

$$(10) \xrightarrow{L.1} (\{\langle x[0] \rangle_l \boxplus \langle c[0] \rangle_r : z_0 |0\rangle |1\rangle - z_1 |1\rangle |0\rangle\}, (a!1.0) \{\emptyset\}_l, \{a?(w).c[0] \leftarrow Z.\text{if}(w)\{c[0] \leftarrow X\}.0\}_r)$$

$$(11) \xrightarrow{r.1} (\{\langle x[0] \rangle_l \boxplus \langle c[0] \rangle_r : z_0 |0\rangle |1\rangle - z_1 |1\rangle |0\rangle\}, (a!1.0) \{\emptyset\}_l, a?(w).c[0] \leftarrow Z.\text{if}(w)\{c[0] \leftarrow X\}.0 \{\emptyset\}_r)$$

...

$$(12) \xrightarrow{L.r.1} (\{\langle x[0] \rangle_l \boxplus \langle c[0] \rangle_r : z_0 |0\rangle |1\rangle - z_1 |1\rangle |0\rangle\}, \{0\}_l, \{c[0] \leftarrow Z.c[0] \leftarrow X.0\}_r)$$

$$(13) \xrightarrow{r.1} (\{\langle x[0] \rangle_l \boxplus \langle c[0] \rangle_r : z_0 |0\rangle |1\rangle + z_1 |1\rangle |0\rangle\}, \{0\}_l, \{c[0] \leftarrow X.0\}_r)$$

$$(14) \xrightarrow{r.1} (\{\langle x[0] \rangle_l \boxplus \langle c[0] \rangle_r : z_0 |0\rangle |0\rangle + z_1 |1\rangle |1\rangle\}, \{0\}_l, \{0\}_r)$$

The above transitions show the last few steps of evaluating Example 7.1. In lines (7) to (12), we transmit two classical bits from membrane l to r through classical message passing. In messaging passing each bit, we first nondeterministically choose to airlock the two membranes through two applications of rule S-MEM, as steps (7) and (8). Since each membrane contains only one process, the probabilities of the choices are 1. We then perform the message communication by rule S-COMM to transmit a message from membrane l to r . Since the choices have been made in (7) and (8), the probability in (9) is 1. Lines (13) and (14) apply two gates to restore the qubit state of $x[1]$ in the new qubit $\langle c[0] \rangle_r$. After the transitions, the entanglement information is transferred from $x[1]$ to $\langle c[0] \rangle_r$, as it is entangled with $x[0]$ now.

7.2 Distributed Quantum Adders

Quantum oracle circuits are reversible and used as subroutines in many quantum algorithms; they usually perform the quantum version of some classical computations, e.g., the oracle component in Shor's algorithm is a quantum version of a modulo-multiplication circuit. They are usually the most resource-consuming component in a quantum circuit [Li et al. 2022] and can be implemented as arithmetic operations based on quantum addition circuits. Distributing the execution of oracle circuits to remote machines can greatly mitigate the entanglement resource needs in a single

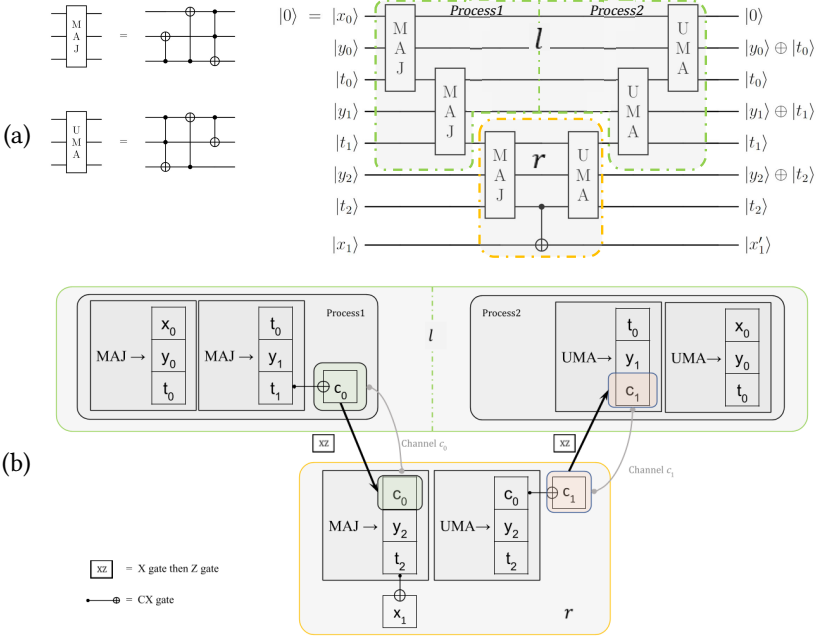


Fig. 9. Ripple-Carry adder circuits. (a): sequential version, (b): distributed version. x'_1 is the overflow bit.

location. Here, we show the example of distributing a quantum ripple-carry adder [Cuccaro et al. 2004]. We also describe the distributing QFT-based adders in Appendix D.

Figure 9a shows the sequential circuit of a three-qubit ripple-carry adder, where we add the value of a three-qubit array t to the value stored in the three-qubit array y , with a two-qubit array x storing extra carry qubits, one for the initial carry and the other for indicating if the addition causes overflow.

$$x[0] \boxplus y[0] \boxplus t[0] \leftarrow \text{MAJ} . x[0] \boxplus y[0] \boxplus t[0] \leftarrow \text{UMA} . 0$$

A quantum ripple-carry adder is constructed by a series of MAJ operations followed by a series of UMA operations, each of which has a diagram on the left side of Figure 9a. To understand the effect of the MAJ and UMA pairs, we show the application of such a pair to qubits $x[0]$, $y[0]$, and $t[0]$ above. Here, $x[0]$ is a carry flag for least significant bits, and $y[0]$ and $t[0]$ are the two bits to add. The application of the MAJ operation adds $t[0]$ to $y[0]$, computes the carry flag for the next significant position, and stores the bit in $t[0]$. The application of the UMA operation reverses the computation in $x[0]$ and $t[0]$ back to their initial bits, but computes the additional result of adding $x[0]$, $y[0]$, and $t[0]$, stored in $y[0]$. As shown in Figure 9a, we arrange the MAJ and UMA sequences in the pattern that every MAJ and UMA pair is placed to connect a carry bit and two bits in the same significant position of arrays y and t . The CX gate in the middle of the circuit produces the overflow flag stored in $x[1]$. We define these steps in DisQ as the following operations.

We distribute the adder to be executed in two membranes l and r , as shown in Figure 9b. Here, we further concurrently execute the two MAJs and UMAs, respectively, through two different processes in l . To enable the communication between l and r , we first re-define the two progresses R and T in Section 7.1, which is used as the two processes in the two membranes of the quantum teleportation circuit, as the parameterized Te and Rt processes below, by permitting qubit input arguments:

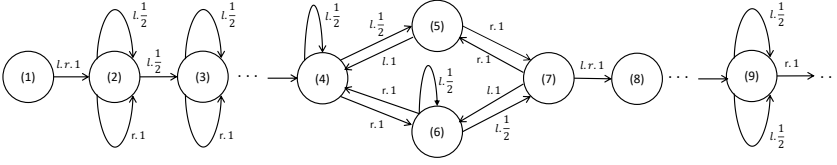


Fig. 10. The adder automaton.

$$\begin{aligned} Te(x, y) &= x \boxplus y \leftarrow CX.x \leftarrow H.u \leftarrow M(x).w \leftarrow M(y).a!u.a!w.0 \\ Rt(x) &= a?(u).a?(w).if(u)\{x \leftarrow Z\}.if(w)\{x \leftarrow X\}.0 \end{aligned}$$

In the Te process, the input argument x represents the quantum qubit waiting to transmit its information to another membrane, and y represents a part of a quantum channel local to a membrane. The input qubit argument x in the Rt process represents the other part of a quantum channel, which stores the transmitted quantum information from the Te process after the teleportation. Below, we define the distributed ripple-carry adder (Figure 9b).

Example 7.2 (Distributed Ripple-Carry Adder). The following program represents a 3-qubit distributed ripple-carry addition circuit and has two membranes l and r . Qubits $x[0]$, $y[0, 2]$, and $t[0, 2]$ belong to membrane l , and qubits $x[1]$, $y[2]$, and $t[2]$ belong to membrane r . Qubit arrays y and t are the input qubits storing two 3-qubit bitstrings as numbers, y stores the final output of adding the two numbers, and $x[0]$ is an ancilla initial carry qubit, $x[1]$ stores the overflow bit.

$$\begin{aligned} \partial c(2). \{x[0] \boxplus y[0] \boxplus t[0] \leftarrow MAJ.t[0] \boxplus y[1] \boxplus t[1] \leftarrow MAJ.Te(u[1], c[0]).0, \\ Rt(c[1]).t[0] \boxplus y[1] \boxplus c[1] \leftarrow UMA.x[0] \boxplus y[0] \boxplus t[0] \leftarrow UMA.0\}_l, \\ \partial c(2). \{Rt(c[0]).c[0] \boxplus y[2] \boxplus t[2] \leftarrow MAJ.t[2] \boxplus x[1] \leftarrow CX.c[0] \boxplus y[2] \boxplus t[2] \leftarrow UMA.Te(c[0], c[1]).0\}_r \end{aligned}$$

In this program, membranes l and r represent different quantum computers. We assume each permits an entanglement of maximal 6 qubits, which means that each computer is not enough to execute the three qubit adder, requiring 8 qubits for execution; so they need to collaborate in executing the adder. We utilize the first process in membrane l to compute the two MAJ applications to y and t , then teleport $t[1]$ to membrane r to compute the addition of the third qubits ($y[2]$ and $t[2]$). The teleportation relies on the quantum channel $\langle c[0] \rangle_l \boxplus \langle c[0] \rangle_r$ and stores $t[1]$'s information in $\langle c[0] \rangle_r$. Membrane r deals with the third qubits with $t[1]$'s information in $\langle c[0] \rangle_r$ and teleports the result carry bit $c[0]$ to the second process in membrane l , via the quantum channel $\langle c[1] \rangle_l \boxplus \langle c[1] \rangle_r$; the $c[0]$ bit is stored in $\langle c[1] \rangle_l$. The second process in membrane r applies the remaining UMA operations. In the procedure of teleporting qubit $t[1]$ to $c[0]$ in membrane r , as well as teleporting qubit $c[0]$ in membrane r to $c[1]$ in membrane l , the $t[1]$ and $c[0]$ qubits are destroyed, so the total number of entangled qubits in every given time of a membrane is less than 6.

To show the equivalence between the sequential ripple-carry adder and its distributed version, we have the following proposition. Since the DisQ simulation can only reason about the measurement results, we assume that the sequential adder and its distributed version are extended with measurement operations at the end to measure all qubits.

PROPOSITION 7.3 (DISTRIBUTED ADDITION SIMULATION). Let Dis-Adder refer to the distributed ripple-carry adder program in Figure 9b and Adder refer to the sequential ripple-carry adder algorithm in Figure 9a, with the qubit array x , y , and t mentioned above. If we equate the measurement result of the qubits $t[1]$ and $\langle c[1] \rangle_l$; thus, Dis-Adder \sqsubseteq Adder.

To understand the simulation in Proposition 7.3, we need to understand the probabilistic transitions in the distributed adder, shown as an automaton in Figure 10. The (1) step creates a two-qubit quantum channel in membranes l and r . The label $l.r.1$ means that we make a non-deterministic

choice in l and r with a probability 1, referring to only one way of making the channel creation. The (2) transition step has three possibilities. The transitions in the second process in l (having a label $l.\frac{1}{2}$) and membrane r (having a label $r.1$) represent airlocks on membranes l and r , respectively, but the airlocks are message receiving operations that are not available at this point; thus, the next very next steps of the two transitions can only perform releasing the airlocks through S-REV. This is why two self-edges point to (2) in Figure 10. The only transition, pushing step (2) to step (3) in the automaton, is the execution of the first process in membrane l (Figure 9b) to execute an MAJ operation. The label $l.\frac{1}{2}$ means that the transition is one of two possible choices in membrane l . The same situation happens in step (3), as an MAJ operation in the first process in l can push the automaton towards the next step.

Steps (4) to (8) in the automaton represent the procedure that passes a classical message from membrane l to r . In step (4), l 's second process is still waiting to receive a message, but l 's first process and membrane r can perform two airlocks, representing a classical communication can be established between the two. Depending on which of the two airlocks performs first, we can transition to either (5) or (6) for performing one of the airlocks, followed by edges from (5) and (6) to (7), indicating the other airlock transition. Since airlocks can be released, we have backward edges from (7) to (5) and (6) and edges from (5) and (6) to (4). The transitions from (7) to (8) commit the message-passing communication between membranes l and r . Transition (9) performs a local action in membrane r . At this point, the prefixed actions in the two processes in membrane l do not change program states, i.e., the first process in l is 0, possibly performing S-SELF, and the second process is waiting to receive a classical message from membrane r . Therefore, we have two self-edges in (9) labeled with l .

The simulation of the sequential and distributed adders' program transitions equates to two sets of program states reaching the same measurement outputs. For every possible measurement output d of executing the sequential adder, having probability p , The above automaton indicates that the sum of probabilities in the sets of program states reaching d is still p because all the different branching cases in executing the distributed version eventually reach the same end goal. In our Java simulation checker, we validate the simulation of the two adders through many test cases.

7.3 Distributed Shor's Algorithm

Shor's algorithm [Shor 1994], a well-known quantum algorithm potentially showing quantum advantages, factorizes a large number, and its core part is the quantum order finding circuit. Unfortunately, the quantum computer power needed for executing Shor's algorithm, such as qubit numbers, surpasses the current quantum computing capability, with some works [Xiao et al. 2023; Yan et al. 2022; Yimsiriwattana and Lomonaco Jr. 2004] thinking of more effective ways of executing the algorithm. Some of these works recognize the power of rewriting Shor's algorithm into distributed versions [Xiao et al. 2023; Yimsiriwattana and Lomonaco Jr. 2004] to save the number of entangled qubits in a single machine. There are two main observations on these algorithms: 1) they tried to distribute the quantum component, the order finding part, and 2) they utilized quantum teleportation to distribute parts of order finding to different machines for execution. These works show one or two special cases of how the algorithm can be distributed.

Here, we show a way of distributing Shor's algorithm through DisQ and show the simulation between the sequential (Figure 11a) and the distributed versions (Figure 11b). Given two n -length qubit arrays $x[0, n]$ and $y[0, n]$, the order finding part (Figure 11a) of Shor's algorithm can be divided into three components: 1) we apply n Hadamard gates H to prepare the superposition state in $x[0, n]$, 2) we use an n step for-loop to apply a controlled- U operation, controlling on $x[j]$ and applying U to $y[0, n]$ for $j \in [0, n]$, each $U(a^{2^j})$ operation applies a modulo-multiplication

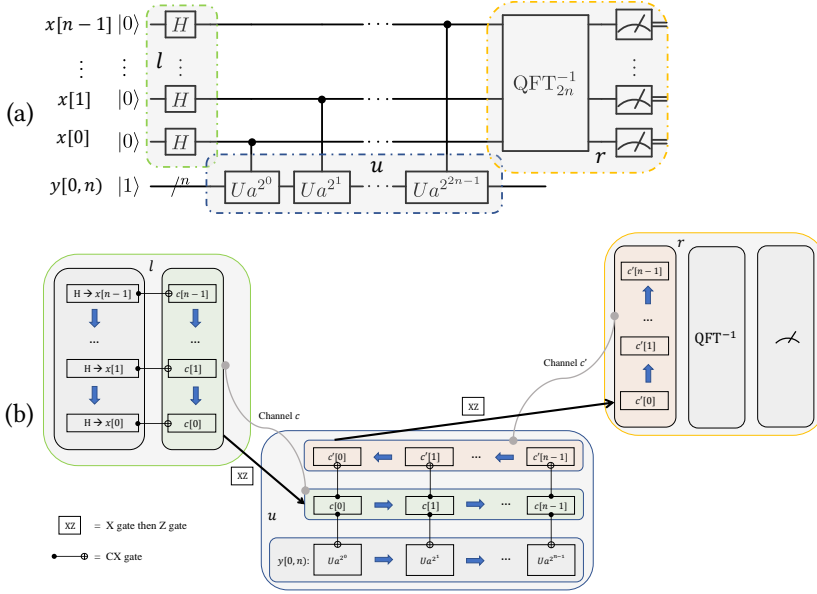


Fig. 11. The quantum order finding circuit of Shor's algorithm. (a): sequential version, (b): distributed version.

$a^{2^j} * y[0, n] \% N$ to the qubit array $y[0, n]$, and 3) we apply QFT^{-1} and measurement, as the phase estimation step, to $x[0, n]$. We now show the distributed version below.

Example 7.4 (Distributed Shor's Algorithm). The following program shows a distributed quantum order finding algorithm, the quantum component of the Shor's algorithm, by using three membranes l , r , and t . Initially, l and r holds n -qubit x and y qubit arrays, respectively, while membrane t does not hold any qubits. $x[0, n]$ has initial state $|0\rangle$, while $y[0, n]$ qubit array has initial state $|1\rangle$. Membranes l and r share an n -qubit quantum channel c , while membranes r and t share an n -qubit quantum channel c' .

Processes:

$$\begin{aligned}
 He(j) &= x[j] \leftarrow H. Te(x[j], c[j]) & HeR(n) &= Rec(0, n, He) \\
 Me(j) &= Rt(c[j]) . c[j] \boxtimes y[0, n] \leftarrow CU(v^{2^j}, N) . Te(c[j], c'[j]) & MeR(n) &= Rec(0, n, Me) \\
 Ed(j) &= Rt(c'[j]) & EdR(n) &= Rec(0, n, Ed)
 \end{aligned}$$

Membranes:

$$\partial c(n) . \{HeR(n)\}_l . \partial c(n) . \partial c'(n) . \{MeR(0)\}_r . \partial c'(n) . \{EdR(n) . c'[0, n] \leftarrow QFT^{-1} . w \leftarrow \mathcal{M}(c'[0, n]) . ps(w)\}_t$$

The above distributed Shor's algorithm is shown as the circuit diagram in Figure 11b. The purpose of the distribution is to put x and y qubit arrays in two different machines, so the entangled qubit numbers are limited to $n + 1$ in each machine. To do so, we create three different membranes l , u , and r to handle the three tasks in the order finding part above. Membrane l is responsible to prepare superposition qubits in x array through the HeR process; we apply a H gate to $\langle x[j] \rangle_l$ and CX gate to the $\langle x[j] \rangle_l$ and $\langle c[j] \rangle_l$ qubits. Membrane u entangles x and y arrays by executing the for-loop through the MeR process; we apply n controlled- U gates between $\langle c[j] \rangle_u$ and the y array to entangle these two and apply n CX gates between the $\langle c[j] \rangle_u$ and $\langle c'[j] \rangle_u$ qubits. Membrane r applies the phase estimation step on the x array through the EdR process; it applies QFT^{-1} and measurement to locus $\langle c'[0, n] \rangle_r$ once $c'[0, n]$ qubits are received.

We now explain the communications among the three membranes. Assuming that two n -length quantum channels c and c' are created, the communications among the three membranes are

managed by c and c' , indicated by the channel edges in Figure 11b, and they are managed in an n -step loop structure; each j -th loop step, we use one qubit Bell pair in the quantum channel c , connecting l and u as $\langle c[j] \rangle_l$ and $\langle c[j] \rangle_u$, to transform the information in $x[j]$ in membrane l to $\langle c[j] \rangle_u$ in membrane u ; such a procedure is finished by single qubit teleportation. The j -th loop step also contains several operations in membrane u . Here, we first apply the controlled- U and CX gates mentioned above, and then perform a single qubit teleportation to transform the information in $\langle c[j] \rangle_u$ to $\langle c'[j] \rangle_r$ in membrane r . The blue arrow in Figure 11b indicates the order of each loop step, including a single qubit teleportation for transforming $\langle x[j] \rangle_l$ to $\langle c[j] \rangle_u$ and another teleportation for transforming $\langle c[j] \rangle_u$ to $\langle c'[j] \rangle_r$. After the communication loop is executed, we then apply the QFT⁻¹ and measurement in membrane r to $\langle c'[0, n] \rangle_r$ at once. The application $ps(w)$ in Example 7.4 refers to the post-processing step after the quantum order funding step.

In every loop step, membrane u only holds $n + 1$ qubits; once the qubit $\langle c[j] \rangle_u$ is destroyed after its information is transferred to membrane r . This discussion omits the fact that the modulo multiplication circuit in membrane u might require many more ancillary qubits, which can be handled based on future circuit distribution, such as the addition circuit distributions in Section 7.2. To equate Shor's algorithm with the distributed version, we have the following proposition. It is trivial to see that the distributed version simulates the original Shor's algorithm since each membrane above contains only one process, i.e., there is no concurrency, and non-determinism is synchronized by classical message passing.

PROPOSITION 7.5 (DISTRIBUTED SHOR'S ALGORITHM SIMULATION). Let Dis-Shors refer to the distributed Shor's program in Figure 11b and Shors refer to the sequential one in Figure 11a, with two n -length input qubit arrays x and y . If we equate the measurement result of x in Shors and the measurement result of the c' array in membrane r in Dis-Shors, thus, Dis-Shors \sqsubseteq Shors.

We test the proposition extensively in our Java simulation checker with many test cases.

8 RELATED WORK

Many previous studies inspire the DISQ development.

Concurrent Quantum Frameworks. Many previous works studied the possibilities of quantum concurrency, in which a quantum program can be partitioned and run in a multi-threaded environment. Ying and Feng [2009] proposed an algebraic logical system to help partition a sequential quantum program into sub-components that can be executed in parallel, blurring providing the properties on how a distributed quantum system can be constructed. Partitioned components might share qubits, which indicates that the proposed partitions represent a concurrent system. Feng et al. [2022] proposes a proof system for concurrent quantum programs based on quantum Hoare logic [Ying 2012]. Ying et al. [2018, 2022] carefully design a quantum concurrent proof system by combining the above two works to permit the concurrent quantum program verification. Zhang and Ying [2024] extended the quantum concurrent proof system with the consideration of atomicity.

Eisert et al. [2000] showed theoretically the resource estimation of implementation a non-local gate, without investigating the forms how long-distance entanglement can be established. Ardeshir-Larijani et al. [2014] developed equivalence checkers for concurrent quantum programs, while Ardeshir-Larijani et al. [2013] developed an equivalence checker for quantum networking protocols.

Quantum Process Algebra. Tafiiovich and Hehner [2009] proposed a framework to specify quantum network protocols. The DISQ's design was inspired by several existing quantum process calculi: qCCS [Feng et al. 2012; Qin et al. 2020; Ying et al. 2009], Communicating Quantum Processes (CQP) [Gay and Nagarajan 2005], quantum model checker (MQC) [Davidson et al. 2012; Gay et al. 2013], QPAI [Jorrand and Lalire 2004], and eQPAI [Haider and Kazmi 2020]. These process calculi are developed to describe quantum networking and security protocols.

Traditional Process Algebra. Communicating Sequential Processes (CSP) [Hoare 1985] and Π -calculus [Milner et al. 1992] are process calculi suitable for defining concurrent systems based on the message-passing model. Several bisimulation and trace-refinement protocol verification methodologies exist for CSP and the Π -calculus [Gibson-Robinson et al. 2014; Ltd. 2010; Sangiorgi 1993]. As noted earlier, the Chemical Abstract Machine [Berry and Boudol 1992] is the inspiration of DisQ.

Quantum Network Protocols and Some Early Distributed Works. Building quantum internet and distributed systems was a long-existing dream for many researchers, with many theoretical and implementation works. For example, [Beals et al. 2013] showed a theory of performing distributed quantum via quantum random access memory. Below, we mainly focus on works showing implementability via NISQ computers. Quantum teleportation [Bennett et al. 1993; Rigolin 2005] serves as the basis for quantum communication between two parties. Julia-Diaz et al. [Juliá-Díaz et al. 2005] provides a two-qubit quantum teleportation protocol. Superdense coding [Bennett and Wiesner 1992] encodes a classical message into a quantum channel. Quantum routing investigates long-distance quantum message transmission, with quantum entanglement swaps being one of the promising protocols for the task [Kozłowski et al. 2020; Pirandola et al. 2017; Wehner et al. 2018]. QPass and QCast are protocols based on the quantum-swap algorithm [Shi and Qian 2020] to maximize the transmission chances through static and semi-dynamic analyses. Researchers developed their circuit implementations [Dahlberg et al. 2019; DiAdamo et al. 2022] and new protocols for enhancing the reliability [Pirker and Dür 2019]. Chakraborty et al. [Chakraborty et al. 2019] provided an alternative protocol for distributed routing. Li et al. [Li et al. 2021] and Caleffi [Caleffi 2017] provide systems to improve transmission chances and message delivery rates. Buhrman and Röhrig [2003] examined the development of distributed quantum computing algorithms, and Cuomo et al. [2023] proposed an optimized compiler for distributed quantum computing.

Single-threaded Quantum Circuit Programming Languages. There are many single-location quantum circuit-based language development. Q# [Svore et al. 2018], Quilc [Smith et al. 2020], Scaffold [JavadiAbhari et al. 2015], Project Q [Steiger et al. 2018], Cirq [Google Quantum AI 2019], Qiskit [Aleksandrowicz et al. 2019] are industrial quantum circuit languages. There are formally verifying quantum circuit programs, including Qwire [Rand 2018], SQIR [Hietala et al. 2021a], and QBricks [Chareton et al. 2021], quantum Hoare logic and its subsequent works [Liu et al. 2019; Ying 2012; Zhou et al. 2023], Qafny [Li et al. 2024]. These tools have been used to verify a range of quantum algorithms, from Grover’s search to quantum phase estimation. There are works verifying quantum circuit optimizations (e.g., voqc [Hietala et al. 2021b], CertiQ [Shi et al. 2019]), as well as verifying quantum circuit compilation procedures, including ReVerC [Amy et al. 2017] and ReQWIRE [Rand et al. 2018]. There are single-location circuit-based equivalence checkers [Chen et al. 2022; Peham et al. 2022; Shi et al. 2020; Sun and Wei 2022; Wang et al. 2022, 2021; Yamashita and Markov 2010] for verifying quantum compiler optimizations.

9 CONCLUSION AND FUTURE WORK

We present DisQ, a system for expressing distributed quantum programs, which are user-specified rewrites of sequential programs. In DisQ, users can rewrite a sequential quantum program to a distributed one that can be executed in a remote distributed quantum system, and DisQ is able to verify their equivalence via the DisQ simulation mechanism. The benefit of such rewrites is to mitigate the restriction of entangled qubit sizes in single-location quantum computers, where we can utilize quantum networking techniques to allow a distributed quantum program to be executed on remote quantum computers where a large entanglement can be built.

We present DisQ’s formal syntax and semantics as a model for a distributed quantum system by combining the CHAM and MDP. We use a type system, with the type soundness, to guarantee that

the execution of `DisQ` program is deadlock-free and represents quantum program behaviors. The `DisQ` simulation relation is measurement-based and developed based on equating sets of program configurations, by summing the probabilities of different branches leading to the same outputs. We show by our case studies that the relation is capable of equating sequential quantum programs and their distributed versions.

Based on `DisQ`, we plan to rewrite different quantum algorithms into distributed versions and develop logical frameworks, such as temporal logics, on top of `DisQ` to reason about sophisticated distributed quantum systems.

ACKNOWLEDGMENTS

This material is based upon work supported by NSF under Award Number 2330974. This paper is dedicated to the memory of our dear co-author Rance Cleaveland.

REFERENCES

- Gadi Aleksandrowicz, Thomas Alexander, Panagiotis Barkoutsos, Luciano Bello, Yael Ben-Haim, David Bucher, Francisco Jose Cabrera-Hernández, Jorge Carballo-Franquis, Adrian Chen, Chun-Fu Chen, Jerry M. Chow, Antonio D. Córcoles-Gonzales, Abigail J. Cross, Andrew Cross, Juan Cruz-Benito, Chris Culver, Salvador De La Puente González, Enrique De La Torre, Delton Ding, Eugene Dumitrescu, Ivan Duran, Pieter Eendebak, Mark Everitt, Ismael Faro Sertage, Albert Frisch, Andreas Fuhrer, Jay Gambetta, Borja Godoy Gago, Juan Gomez-Mosquera, Donny Greenberg, Ikko Hamamura, Vojtech Havlicek, Joe Hellmers, Lukasz Herok, Hiroshi Horii, Shaohan Hu, Takashi Imamichi, Toshinari Itoko, Ali Javadi-Abhari, Naoki Kanazawa, Anton Karazeev, Kevin Krsulich, Peng Liu, Yang Luh, Yunho Maeng, Manoel Marques, Francisco Jose Martín-Fernández, Douglas T. McClure, David McKay, Srujan Meesala, Antonio Mezzacapo, Nikolaj Moll, Diego Moreda Rodríguez, Giacomo Nannicini, Paul Nation, Pauline Ollitrault, Lee James O’Riordan, Hanhee Paik, Jesús Pérez, Anna Phan, Marco Pistoia, Viktor Prutyaynov, Max Reuter, Julia Rice, Abdón Rodríguez Davila, Raymond Harry Putra Rudy, Mingi Ryu, Ninad Sathaye, Chris Schnabel, Eddie Schoute, Kanav Setia, Yunong Shi, Adenilton Silva, Yukio Siraichi, Seyon Sivarajah, John A. Smolin, Mathias Soeken, Hitomi Takahashi, Ivano Tavernelli, Charles Taylor, Pete Taylour, Kenso Trabling, Matthew Treinish, Wes Turner, Desiree Vogt-Lee, Christophe Vuillot, Jonathan A. Wildstrom, Jessica Wilson, Erick Winston, Christopher Wood, Stephen Wood, Stefan Wörner, Ismail Yunus Akhalwaya, and Christa Zoufal. 2019. Qiskit: An open-source framework for quantum computing. <https://doi.org/10.5281/zenodo.2562110>
- A. Ambainis. 2004. Quantum walk algorithm for element distinctness. In *45th Annual IEEE Symposium on Foundations of Computer Science*. 22–31. <https://doi.org/10.1109/FOCS.2004.54>
- Matthew Amy, Martin Roetteler, and Krysta M. Svore. 2017. Verified Compilation of Space-Efficient Reversible Circuits. In *Computer Aided Verification*, Rupak Majumdar and Viktor Kunčák (Eds.). Springer International Publishing, Cham, 3–21.
- Ebrahim Ardeshir-Larijani, Simon J. Gay, and Rajagopal Nagarajan. 2013. Equivalence Checking of Quantum Protocols. In *Tools and Algorithms for the Construction and Analysis of Systems*, Nir Piterman and Scott A. Smolka (Eds.). Springer Berlin Heidelberg, Berlin, Heidelberg, 478–492.
- Ebrahim Ardeshir-Larijani, Simon J. Gay, and Rajagopal Nagarajan. 2014. Verification of Concurrent Quantum Protocols by Equivalence Checking. In *Tools and Algorithms for the Construction and Analysis of Systems*, Erika Ábrahám and Klaus Havelund (Eds.). Springer Berlin Heidelberg, Berlin, Heidelberg, 500–514.
- David Barral, F. Javier Cardama, Guillermo Díaz, Daniel Faílde, Iago F. Llovo, Mariamo Mussa Juane, Jorge Vázquez-Pérez, Juan Villaso, César Piñeiro, Natalia Costas, Juan C. Pichel, Tomás F. Pena, and Andrés Gómez. 2024. Review of Distributed Quantum Computing. From single QPU to High Performance Quantum Computing. arXiv:2404.01265 [quant-ph]
- Samik Basu, Madhavan Mukund, C. R. Ramakrishnan, I. V. Ramakrishnan, and Rakesh Verma. 2001. Local and Symbolic Bisimulation Using Tabled Constraint Logic Programming. In *Logic Programming*, Philippe Codognet (Ed.). Springer Berlin Heidelberg, Berlin, Heidelberg, 166–180.
- Robert Beals, Stephen Brierley, Oliver Gray, Aram W. Harrow, Samuel Kutin, Noah Linden, Dan Shepherd, and Mark Stather. 2013. Efficient distributed quantum computing. *Proceedings of the Royal Society A: Mathematical, Physical and Engineering Sciences* 469, 2153 (May 2013), 20120686. <https://doi.org/10.1098/rspa.2012.0686>
- Stephane Beauregard. 2003. Circuit for Shor’s Algorithm Using $2n+3$ Qubits. *Quantum Info. Comput.* 3, 2 (March 2003), 175–185.
- Charles H. Bennett, Gilles Brassard, Claude Crépeau, Richard Jozsa, Asher Peres, and William K. Wootters. 1993. Teleporting an unknown quantum state via dual classical and Einstein-Podolsky-Rosen channels. *Phys. Rev. Lett.* 70 (Mar 1993), 1895–1899. Issue 13. <https://doi.org/10.1103/PhysRevLett.70.1895>

- Charles H. Bennett and Stephen J. Wiesner. 1992. Communication via one- and two-particle operators on Einstein-Podolsky-Rosen states. *Phys. Rev. Lett.* 69 (Nov 1992), 2881–2884. Issue 20. <https://doi.org/10.1103/PhysRevLett.69.2881>
- G rard Berry and G rard Boudol. 1992. The chemical abstract machine. *Theoretical Computer Science* 96, 1 (1992), 217–248. [https://doi.org/10.1016/0304-3975\(92\)90185-1](https://doi.org/10.1016/0304-3975(92)90185-1)
- Anita Buckley, Pavel Chuprikov, Rodrigo Otoni, Robert Rand, Robert Soul , and Patrick Eugster. 2024. An Algebraic Language for Specifying Quantum Networks. In *PLDI 2024*.
- Harry Buhrman and Hein R hrig. 2003. Distributed Quantum Computing. 1–20. https://doi.org/10.1007/978-3-540-45138-9_1
- Marcello Caleffi. 2017. Optimal Routing for Quantum Networks. *IEEE Access* 5 (2017), 22299–22312. <https://doi.org/10.1109/ACCESS.2017.2763325>
- Marcello Caleffi, Michele Amoretti, Davide Ferrari, Daniele Cuomo, Jessica Illiano, Antonio Manzalini, and Angela Sara Cacciapuoti. 2022. Distributed Quantum Computing: a Survey. (12 2022). arXiv:2212.10609 [quant-ph]
- Kaushik Chakraborty, Filip Rozpedek, Axel Dahlberg, and Stephanie Wehner. 2019. Distributed Routing in a Quantum Internet. <https://doi.org/10.48550/ARXIV.1907.11630>
- Christophe Charetton, S bastien Bardin, Fran ois Bobot, Valentin Perrelle, and Beno t Valiron. 2021. An Automated Deductive Verification Framework for Circuit-building Quantum Programs. In *Programming Languages and Systems - 30th European Symposium on Programming, ESOP 2021, Held as Part of the European Joint Conferences on Theory and Practice of Software, ETAPS 2021, Luxembourg City, Luxembourg, March 27 - April 1, 2021, Proceedings (Lecture Notes in Computer Science, Vol. 12648)*, Nobuko Yoshida (Ed.), Springer, 148–177. https://doi.org/10.1007/978-3-030-72019-3_6
- Tian-Fu Chen, Jie-Hong R. Jiang, and Min-Hsiu Hsieh. 2022. Partial Equivalence Checking of Quantum Circuits. In *2022 IEEE International Conference on Quantum Computing and Engineering (QCE)*. IEEE. <https://doi.org/10.1109/qce53715.2022.00082>
- Andrew Childs, Ben Reichardt, Robert Spalek, and Shengyu Zhang. 2007. Every NAND formula of size N can be evaluated in time $N^{1/2+o(1)}$ on a Quantum Computer. (03 2007).
- Steven Cuccaro, Thomas Draper, Samuel Kutin, and David Moulton. 2004. A new quantum ripple-carry addition circuit. (11 2004).
- Daniele Cuomo, Marcello Caleffi, and Angela Sara Cacciapuoti. 2020. Towards a distributed quantum computing ecosystem. *IET Quantum Communication* 1, 1 (July 2020), 3–8. <https://doi.org/10.1049/iet-qtc.2020.0002>
- Daniele Cuomo, Marcello Caleffi, Kevin Krsulich, Filippo Tramonto, Gabriele Agliardi, Enrico Prati, and Angela Sara Cacciapuoti. 2023. Optimized Compiler for Distributed Quantum Computing. *ACM Transactions on Quantum Computing* 4, 2, Article 15 (feb 2023), 29 pages. <https://doi.org/10.1145/3579367>
- Axel Dahlberg, Matthew Skrzypczyk, Tim Coopmans, Leon Wubben, Filip Rozpundefneddek, Matteo Pompili, Arian Stolk, Przemyslaw Pawelczak, Robert Knegjens, Julio de Oliveira Filho, Ronald Hanson, and Stephanie Wehner. 2019. A Link Layer Protocol for Quantum Networks. In *Proceedings of the ACM Special Interest Group on Data Communication (Beijing, China) (SIGCOMM '19)*. Association for Computing Machinery, New York, NY, USA, 159–173. <https://doi.org/10.1145/3341302.3342070>
- Zohreh Davarzani, Mariam Zomorodi, and Mahboobeh Houshmand. 2022. A Hierarchical Approach For Building Distributed Quantum Systems. *Scientific Reports* 12 (09 2022). <https://doi.org/10.1038/s41598-022-18989-w>
- Tim Davidson, Simon Gay, H. Mlna rik, Rajagopal Nagarajan, and Nick Papanikolaou. 2012. Model Checking for Communicating Quantum Processes. *International Journal of Unconventional Computing* 8 (01 2012), 73–98.
- Stephen DiAdamo, Marco Ghibaudi, and James Cruise. 2021. Distributed Quantum Computing and Network Control for Accelerated VQE. *IEEE Transactions on Quantum Engineering* 2 (2021), 1–21. <https://doi.org/10.1109/tqe.2021.3057908>
- Stephen DiAdamo, Bing Qi, Glen Miller, Ramana Kompella, and Alireza Shabani. 2022. Packet switching in quantum networks: A path to the quantum Internet. *Phys. Rev. Res.* 4 (Oct 2022), 043064. Issue 4. <https://doi.org/10.1103/PhysRevResearch.4.043064>
- Paul Adrien Maurice Dirac. 1939. A new notation for quantum mechanics. *Mathematical Proceedings of the Cambridge Philosophical Society* 35 (1939), 416 – 418.
- Duncan Earl, K. Karunaratne, Jason Schaaqe, Ryan Strum, Patrick Swingle, and Ryan Wilson. 2022. Architecture of a First-Generation Commercial Quantum Network. (11 2022). arXiv:2211.14871 [quant-ph]
- J. Eisert, K. Jacobs, P. Papadopoulos, and M. B. Plenio. 2000. Optimal local implementation of nonlocal quantum gates. *Phys. Rev. A* 62 (Oct 2000), 052317. Issue 5. <https://doi.org/10.1103/PhysRevA.62.052317>
- Yuan Feng, Runyao Duan, and Mingsheng Ying. 2012. Bisimulation for Quantum Processes. *ACM Trans. Program. Lang. Syst.* 34, 4, Article 17 (dec 2012), 43 pages. <https://doi.org/10.1145/2400676.2400680>
- Yuan Feng, Sanjiang Li, and Mingsheng Ying. 2022. Verification of Distributed Quantum Programs. *ACM Trans. Comput. Logic* 23, 3, Article 19 (apr 2022), 40 pages. <https://doi.org/10.1145/3517145>
- Simon Gay, Rajagopal Nagarajan, and Nikolaos Papanikolaou. 2013. Specification and Verification of Quantum Protocols. *Semantic Techniques in Quantum Computation* (01 2013). <https://doi.org/10.1017/CBO9781139193313.012>

- Simon J. Gay and Rajagopal Nagarajan. 2005. Communicating Quantum Processes. In *Proceedings of the 32nd ACM SIGPLAN-SIGACT Symposium on Principles of Programming Languages* (Long Beach, California, USA) (POPL '05). Association for Computing Machinery, New York, NY, USA, 145–157. <https://doi.org/10.1145/1040305.1040318>
- Radu-Iulian Gheorghica. 2023. An Algorithm for Concurrent Use of Quantum Simulators and Computers in the Context of Subgraph Isomorphism. In *2023 IEEE 17th International Symposium on Applied Computational Intelligence and Informatics (SACI)*. 000721–000726. <https://doi.org/10.1109/SACI58269.2023.10158547>
- Thomas Gibson-Robinson, Alexandre Boulgakov Philip Armstrong, and A.W. Roscoe. 2014. FDR3 - A Modern Refinement Checker for CSP. In *TACAS*. In Press.
- Google Quantum AI. 2019. Cirq: An Open Source Framework for Programming Quantum Computers. <https://quantumai.google/cirq>
- Fabrizio Granelli, Riccardo Bassoli, Janis Nötzel, Frank Fitzek, Holger Boche, and Nelson Fonseca. 2022. A Novel Architecture for Future Classical-Quantum Communication Networks. *Wireless Communications and Mobile Computing* 2022 (04 2022), 1–18. <https://doi.org/10.1155/2022/3770994>
- Daniel M. Greenberger, Michael A. Horne, and Anton Zeilinger. 1989. *Going beyond Bell's Theorem*. Springer Netherlands, Dordrecht, 69–72. https://doi.org/10.1007/978-94-017-0849-4_10
- Salman Haider and Dr. Syed Asad Raza Kazmi. 2020. An extended quantum process algebra (eQPAI_g) approach for distributed quantum systems. arXiv:2001.04249 [cs.LO]
- Thomas Häner, Vadym Kliuchnikov, Martin Roetteler, Mathias Soeken, and Alexander Vaschillo. 2022. QParallel: Explicit Parallelism for Programming Quantum Computers. (10 2022). arXiv:2210.03680 [quant-ph]
- Thomas Häner, Martin Roetteler, and Krysta M. Svore. 2017. Factoring Using $2n + 2$ Qubits with Toffoli Based Modular Multiplication. *Quantum Info. Comput.* 17, 7–8 (June 2017), 673–684.
- Thomas Häner, Damian S. Steiger, Torsten Hoefler, and Matthias Troyer. 2021. Distributed quantum computing with QMPI. In *Proceedings of the International Conference for High Performance Computing, Networking, Storage and Analysis* (, St. Louis, Missouri,) (SC '21). Association for Computing Machinery, New York, NY, USA, Article 16, 13 pages. <https://doi.org/10.1145/3458817.3476172>
- Kesha Hietala, Robert Rand, Shih-Han Hung, Liyi Li, and Michael Hicks. 2021a. Proving Quantum Programs Correct. In *Proceedings of the Conference on Interactive Theorem Proving (ITP)*.
- Kesha Hietala, Robert Rand, Shih-Han Hung, Xiaodi Wu, and Michael Hicks. 2021b. A Verified Optimizer for Quantum Circuits. In *Proceedings of the ACM Conference on Principles of Programming Languages (POPL)*.
- Stefan Hillmich, Alwin Zulehner, and Robert Wille. 2020. Concurrency in DD-based Quantum Circuit Simulation. In *2020 25th Asia and South Pacific Design Automation Conference (ASP-DAC)*. 115–120. <https://doi.org/10.1109/ASP-DAC47756.2020.9045711>
- C. A. R. Hoare. 1985. *Communicating sequential processes*. Prentice-Hall, Inc., Upper Saddle River, NJ, USA.
- Photonic Inc, Francis Afzal, Mohsen Akhlaghi, Stefanie J. Beale, Olinka Bedroya, Kristin Bell, Laurent Bergeron, Kent Bonsma-Fisher, Polina Bychkova, Zachary M. E. Chaisson, Camille Chartrand, Chloe Clear, Adam Darcie, Adam DeAbreu, Colby DeLisle, Lesley A. Duncan, Chad Dundas Smith, John Dunne, Amir Ebrahimi, Nathan Evetts, Daker Fernandes Pinheiro, Patricio Fuentes, Tristen Georgiou, Biswarup Guha, Rafael Haenel, Daniel Higginbottom, Daniel M. Jackson, Navid Jahed, Amin Khorshidahmad, Prasoon K. Shandilya, Alexander T. K. Kurkjian, Nikolai Lauk, Nicholas R. Lee-Hone, Eric Lin, Rostyslav Litynskyy, Duncan Lock, Lisa Ma, Iain MacGilp, Evan R. MacQuarrie, Aaron Mar, Alireza Marefat Khah, Alex Matias, Evan Meyer-Scott, Cathryn P. Michaels, Juliana Motira, Narwan Kabir Noori, Egor Ospadov, Ekta Patel, Alexander Patscheider, Danny Paulson, Ariel Petruk, Adarsh L. Ravindranath, Bogdan Reznichenko, Myles Ruether, Jeremy Ruscica, Kunal Saxena, Zachary Schaller, Alex Seidlitz, John Senger, Youn Seok Lee, Orbel Sevoyan, Stephanie Simmons, Oney Soykal, Leea Stott, Quyen Tran, Spyros Tserkis, Ata Ulhaq, Wyatt Vine, Russ Weeks, Gary Wolfowicz, and Isao Yoneda. 2024. Distributed Quantum Computing in Silicon. arXiv:2406.01704 [quant-ph]
- Ali JavadiAbhari, Shruti Patil, Daniel Kudrow, Jeff Heckey, Alexey Lvov, Frederic T. Chong, and Margaret Martonosi. 2015. ScaffCC: Scalable compilation and analysis of quantum programs. *Parallel Comput.* 45 (June 2015), 2–17. <https://doi.org/10.1016/j.parco.2014.12.001>
- Philippe Jorrand and Marie Lalire. 2004. Toward a Quantum Process Algebra. In *Proceedings of the 1st Conference on Computing Frontiers* (Ischia, Italy) (CF '04). Association for Computing Machinery, New York, NY, USA, 111–119. <https://doi.org/10.1145/977091.977108>
- B. Juliá-Díaz, Joseph Burdis, and Frank Tabakin. 2005. QDENSIT—a mathematica quantum computer simulation. *Computer Physics Communications* 180 (08 2005), 914–934. <https://doi.org/10.1016/j.cpc.2005.12.021>
- Wojciech Kozłowski, Axel Dahlberg, and Stephanie Wehner. 2020. Designing a Quantum Network Protocol. In *Proceedings of the 16th International Conference on Emerging Networking Experiments and Technologies* (Barcelona, Spain) (CoNEXT '20). Association for Computing Machinery, New York, NY, USA, 1–16. <https://doi.org/10.1145/3386367.3431293>
- Dario Lago-Rivera, Jelena V. Rakonjac, Samuele Grandi, and Hugues de Riedmatten. 2023. Long distance multiplexed quantum teleportation from a telecom photon to a solid-state qubit. *Nature Communications* 14, 1 (05 Apr 2023), 1889.

<https://doi.org/10.1038/s41467-023-37518-5>

- Jian Li, Mingjun Wang, Qidong Jia, Kaiping Xue, Nenghai Yu, Qibin Sun, and Jun Lu. 2021. Fidelity-Guarantee Entanglement Routing in Quantum Networks. <https://doi.org/10.48550/ARXIV.2111.07764>
- Liyi Li, Finn Voichick, Kesha Hietala, Yuxiang Peng, Xiaodi Wu, and Michael Hicks. 2022. Verified Compilation of Quantum Oracles. In *OOPSLA 2022*. <https://doi.org/10.48550/ARXIV.2112.06700>
- Liyi Li, Mingwei Zhu, Rance Cleaveland, Alexander Nicoletlis, Yi Lee, Le Chang, and Xiaodi Wu. 2024. Qafny: A Quantum-Program Verifier. In *ECOOP 2024*.
- Junyi Liu, Bohua Zhan, Shuling Wang, Shenggang Ying, Tao Liu, Yangjia Li, Mingsheng Ying, and Naijun Zhan. 2019. Formal Verification of Quantum Algorithms Using Quantum Hoare Logic. In *Computer Aided Verification*, Isil Dillig and Serdar Tasiran (Eds.). Springer International Publishing, Cham, 187–207.
- Formal Systems (Europe) Ltd. 2010. Failures-Divergence Refinement. FDR2 User Manual. In *FDR2 User Manual*.
- Frédéric Magniez, Miklos Santha, and Mario Szegedy. 2005. Quantum Algorithms for the Triangle Problem. In *Proceedings of the Sixteenth Annual ACM-SIAM Symposium on Discrete Algorithms (Vancouver, British Columbia) (SODA '05)*. Society for Industrial and Applied Mathematics, USA, 1109–1117.
- Andrey Markov. 1906. Rasprostranenie zakona bol'shih chisel na velichiny, zavisyaschie drug ot druga. *Izvestiya Fiziko-matematicheskogo obschestva pri Kazanskom universitete* 15 (1906), 135–156.
- Andrey Markov. 1907. Extension of the Limit Theorems of Probability Theory to a Sum of Variables Connected in a chain. *The Notes of the Imperial Academy of Sciences of St. Petersburg VIII Series, Physio-Mathematical College XXII/9* (1907).
- R. Van Meter and S. J. Devitt. 2016. The Path to Scalable Distributed Quantum Computing. *Computer* 49, 09 (sep 2016), 31–42. <https://doi.org/10.1109/MC.2016.291>
- Robin Milner. 1980. *A Calculus of Communicating Systems*. Springer Berlin, Heidelberg.
- Robin Milner, Joachim Parrow, and David Walker. 1992. A calculus of mobile processes, I. *Information and Computation* 100, 1 (1992), 1–40. [https://doi.org/10.1016/0890-5401\(92\)90008-4](https://doi.org/10.1016/0890-5401(92)90008-4)
- Sreraman Muralidharan. 2024. The simulation of distributed quantum algorithms. arXiv:2402.10745 [quant-ph]
- Michael A. Nielsen and Isaac L. Chuang. 2011. *Quantum Computation and Quantum Information* (10th anniversary ed.). Cambridge University Press, USA.
- Karmela Padavic-Callaghan. 2023. *Record-breaking Number of Qubits Entangled In a Quantum Computer*. <https://www.newscientist.com/article/2382022-record-breaking-number-of-qubits-entangled-in-a-quantum-computer/>
- Rhea Parekh, Andrea Ricciardi, Ahmed Darwish, and Stephen DiAdamo. 2021. Quantum Algorithms and Simulation for Parallel and Distributed Quantum Computing. In *2021 IEEE/ACM Second International Workshop on Quantum Computing Software (QCS)*. 9–19. <https://doi.org/10.1109/QCS54837.2021.00005>
- Tom Peham, Lukas Burgholzer, and Robert Wille. 2022. Equivalence Checking of Quantum Circuits With the ZX-Calculus. *IEEE Journal on Emerging and Selected Topics in Circuits and Systems* 12, 3 (Sept. 2022), 662–675. <https://doi.org/10.1109/jetcas.2022.3202204>
- S. Pirandola, J. Eisert, C. Weedbrook, A. Furusawa, and S. L. Braunstein. 2015. Advances in quantum teleportation. *Nature Photonics* 9, 10 (01 Oct 2015), 641–652. <https://doi.org/10.1038/nphoton.2015.154>
- Stefano Pirandola, Riccardo Laurenza, Carlo Ottaviani, and Leonardo Banchi. 2017. Fundamental limits of repeaterless quantum communications. *Nature Communications* 8 (04 2017), 15043. <https://doi.org/10.1038/ncomms15043>
- A Pirker and W Dür. 2019. A quantum network stack and protocols for reliable entanglement-based networks. *New Journal of Physics* 21, 3 (mar 2019), 033003. <https://doi.org/10.1088/1367-2630/ab05f7>
- Martin L. Puterman. 1994. *Markov Decision Processes: Discrete Stochastic Dynamic Programming* (1st ed.). John Wiley & Sons, Inc., USA.
- Matthew Pysher, Alon Bahabad, Peng Peng, Ady Arie, and Olivier Pfister. 2010. Quasi-phase-matched concurrent nonlinearities in periodically poled KTiOPO4 for quantum computing over the optical frequency comb. *Opt. Lett.* 35, 4 (Feb 2010), 565–567. <https://doi.org/10.1364/OL.35.000565>
- Xudong Qin, Yuxin Deng, and Wenjie Du. 2020. Verifying Quantum Communication Protocols with Ground Bisimulation. In *Tools and Algorithms for the Construction and Analysis of Systems*, Armin Biere and David Parker (Eds.). Springer International Publishing, Cham, 21–38.
- Robert Rand. 2018. *Formally verified quantum programming*. Ph.D. Dissertation. University of Pennsylvania.
- Robert Rand, Jennifer Paykin, Dong-Ho Lee, and S. Zdancewic. 2018. ReQWIRE: Reasoning about Reversible Quantum Circuits. In *QPL*.
- Gustavo Rigolin. 2005. Quantum teleportation of an arbitrary two-qubit state and its relation to multipartite entanglement. *Physical Review A* 71, 3 (mar 2005). <https://doi.org/10.1103/physreva.71.032303>
- Davide Sangiorgi. 1993. A Theory of Bisimulation for the pi-Calculus. In *CONCUR (Lecture Notes in Computer Science, Vol. 715)*, Eike Best (Ed.). Springer, 127–142.
- Shouqian Shi and Chen Qian. 2020. Concurrent Entanglement Routing for Quantum Networks: Model and Designs. In *Proceedings of the Annual Conference of the ACM Special Interest Group on Data Communication on the Applications*,

- Technologies, Architectures, and Protocols for Computer Communication* (Virtual Event, USA) (SIGCOMM '20). Association for Computing Machinery, New York, NY, USA, 62–75. <https://doi.org/10.1145/3387514.3405853>
- Yunong Shi, Xupeng Li, Runzhou Tao, Ali Javadi-Abhari, Andrew W. Cross, Frederic T. Chong, and Ronghui Gu. 2019. Contract-based verification of a realistic quantum compiler. *arXiv e-prints* (Aug 2019). arXiv:1908.08963 [quant-ph]
- Yunong Shi, Runzhou Tao, Xupeng Li, Ali Javadi-Abhari, Andrew W. Cross, Frederic T. Chong, and Ronghui Gu. 2020. CertiQ: A Mostly-automated Verification of a Realistic Quantum Compiler. arXiv:1908.08963 [quant-ph]
- P.W. Shor. 1994. Algorithms for quantum computation: discrete logarithms and factoring. In *Proceedings 35th Annual Symposium on Foundations of Computer Science*. 124–134. <https://doi.org/10.1109/SFCS.1994.365700>
- Robert S. Smith, Eric C. Peterson, Mark G. Skilbeck, and Erik J. Davis. 2020. An Open-Source, Industrial-Strength Optimizing Compiler for Quantum Programs. arXiv:2003.13961 [quant-ph]
- Damian S. Steiger, Thomas Häner, and Matthias Troyer. 2018. ProjectQ: an open source software framework for quantum computing. *Quantum* 2 (Jan. 2018), 49. <https://doi.org/10.22331/q-2018-01-31-49>
- Weixiao Sun and Zhaohui Wei. 2022. Equivalence checking of quantum circuits by nonlocality. *npj Quantum Information* 8, 1 (29 Nov 2022), 139. <https://doi.org/10.1038/s41534-022-00652-x>
- Krysta Svore, Alan Geller, Matthias Troyer, John Azariah, Christopher Granade, Bettina Heim, Vadym Kliuchnikov, Mariia Mykhailova, Andres Paz, and Martin Roetteler. 2018. Q#: Enabling Scalable Quantum Computing and Development with a High-level DSL. In *Proceedings of the Real World Domain Specific Languages Workshop 2018 (RWDSL2018)*. ACM. <https://doi.org/10.1145/3183895.3183901>
- Anya Tafliovich and Eric C.R. Hehner. 2009. Programming with Quantum Communication. *Electronic Notes in Theoretical Computer Science* 253, 3 (2009), 99–118. <https://doi.org/10.1016/j.entcs.2009.10.008> Proceedings of Seventh Workshop on Quantitative Aspects of Programming Languages (QAPL 2009).
- Wei Tang and Margaret Martonosi. 2024. Distributed Quantum Computing via Integrating Quantum and Classical Computing. *Computer* 57, 4 (2024), 131–136. <https://doi.org/10.1109/MC.2024.3360569>
- R. S. Tessinari, R. I. Woodward, and A. J. Shields. 2023. Software-Defined Quantum Network Using a QKD-Secured SDN Controller and Encrypted Messages, In *Optical Fiber Communication Conference (OFC) 2023*. *Optical Fiber Communication Conference (OFC) 2023*, W2A.38. <https://doi.org/10.1364/OFC.2023.W2A.38>
- Qisheng Wang, Riling Li, and Mingsheng Ying. 2022. Equivalence Checking of Sequential Quantum Circuits. *IEEE Transactions on Computer-Aided Design of Integrated Circuits and Systems* 41, 9 (Sept. 2022), 3143–3156. <https://doi.org/10.1109/tcad.2021.3117506>
- Qisheng Wang, Junyi Liu, and Mingsheng Ying. 2021. Equivalence checking of quantum finite-state machines. *J. Comput. System Sci.* 116 (March 2021), 1–21. <https://doi.org/10.1016/j.jcss.2020.08.004>
- Stephanie Wehner, David Elkouss, and Ronald Hanson. 2018. Quantum internet: A vision for the road ahead. *Science* 362, 6412 (2018), eaam9288. <https://doi.org/10.1126/science.aam9288> arXiv:<https://www.science.org/doi/pdf/10.1126/science.aam9288>
- Ligang Xiao, Daowen Qiu, Le Luo, and Paulo Mateus. 2023. Distributed Shor’s algorithm. *Quantum Information and Computation* 23 (01 2023), 27–44. <https://doi.org/10.26421/QIC23.1-2-3>
- Shigeru Yamashita and Igor L. Markov. 2010. Fast equivalence-checking for quantum circuits. In *2010 IEEE/ACM International Symposium on Nanoscale Architectures*. 23–28. <https://doi.org/10.1109/NANOARCH.2010.5510932>
- Bao Yan, Ziqi Tan, Shijie Wei, Haocong Jiang, Weilong Wang, Hong Wang, Lan Luo, Qianheng Duan, Yiting Liu, Wenhao Shi, Yangyang Fei, Xiangdong Meng, Yu Han, Zheng Shan, Jiachen Chen, Xuhao Zhu, Chuanyu Zhang, Feitong Jin, Hekang Li, Chao Song, Zhen Wang, Zhi Ma, H. Wang, and Gui-Lu Long. 2022. Factoring integers with sublinear resources on a superconducting quantum processor. arXiv:2212.12372 [quant-ph]
- Anocha Yimsiriwattana and Samuel J. Lomonaco Jr. 2004. Distributed quantum computing: a distributed Shor algorithm. In *Quantum Information and Computation II*, Eric Donkor, Andrew R. Pirich, and Howard E. Brandt (Eds.). SPIE. <https://doi.org/10.1117/12.546504>
- Mingsheng Ying. 2012. Floyd–Hoare Logic for Quantum Programs. *ACM Trans. Program. Lang. Syst.* 33, 6, Article 19 (Jan. 2012), 49 pages. <https://doi.org/10.1145/2049706.2049708>
- Mingsheng Ying and Yuan Feng. 2009. An Algebraic Language for Distributed Quantum Computing. *IEEE Trans. Comput.* 58, 6 (2009), 728–743. <https://doi.org/10.1109/TC.2009.13>
- Mingsheng Ying, Yuan Feng, Runyao Duan, and Zhengfeng Ji. 2009. An Algebra of Quantum Processes. *ACM Trans. Comput. Logic* 10, 3, Article 19 (apr 2009), 36 pages. <https://doi.org/10.1145/1507244.1507249>
- Mingsheng Ying, Li Zhou, and Yangjia Li. 2018. Reasoning about Parallel Quantum Programs. arXiv:1810.11334
- Mingsheng Ying, Li Zhou, Yangjia Li, and Yuan Feng. 2022. A proof system for disjoint parallel quantum programs. *Theoretical Computer Science* 897 (2022), 164–184. <https://doi.org/10.1016/j.tcs.2021.10.025>
- Zhicheng Zhang and Mingsheng Ying. 2024. Atomicity in Distributed Quantum Computing. arXiv:2404.18592 [quant-ph]
- Li Zhou, Gilles Barthe, Pierre-Yves Strub, Junyi Liu, and Mingsheng Ying. 2023. CoqQ: Foundational Verification of Quantum Programs. *Proc. ACM Program. Lang.* 7, POPL, Article 29 (jan 2023), 33 pages. <https://doi.org/10.1145/3571222>

A DISQ KIND CHECKING

$$\begin{array}{c}
\frac{\Omega(x) = C}{\Omega \vdash x : \Omega(x)} \quad \frac{\Omega \vdash a_1 : C \quad \Omega \vdash a_2 : C}{\Omega \vdash a_1 + a_2 : C} \quad \frac{\Omega \vdash a_1 : C \quad \Omega \vdash a_2 : C}{\Omega \vdash a_1 \cdot a_2 : C} \quad \frac{\Omega \vdash a_1 : C \quad \Omega \vdash a_2 : C}{\Omega \vdash a_1 = a_2 : C} \\
\\
\frac{\Omega \vdash a_1 : C \quad \Omega \vdash a_2 : C}{\Omega \vdash a_1 < a_2 : C} \quad \frac{\Omega \vdash b : C}{\Omega \vdash \neg b : C}
\end{array}$$

Fig. 12. Arith and Bool Kind Checking

The kind checking procedure $\Omega \vdash - : C$ verifies if $-$ is a C kind term, based on the kind checking in [Li et al. 2024], and the rules for arithmetic and Boolean expressions are in Figure 12. The construct $-$ here refers to arithmetic, Boolean equations, or a statement.

B DISQ EQUIVALENCE RELATIONS

The DisQ type system maintains simultaneity through the type-guided state rewrites, formalized as equivalence relations (Figure 8). We only show the rewrite rules for local loci, and the loci with membrane structures can be manipulated through the merged rules in Figure 3, as well as a similar style of permutation rules in Section 4.3. Other than the locus qubit position permutation being introduced, the types below associated with loci in the environment also play an essential role in the rewrites.

| | | | | | | |
|-----------------------|------------|-----|--|---|--|--------------------|
| Quantum Type | $\tau ::=$ | Nor | | Had | | EN |
| Quantum Value (Forms) | $q ::=$ | w | | $\frac{1}{\sqrt{2^n}} \otimes_{j=0}^{n-1} (0\rangle + \alpha(r_j) 1\rangle)$ | | $\sum_{j=0}^m w_j$ |

The DisQ type system is inherited from the QAFNY type system [Li et al. 2024] with three different types. Quantum values are categorized into three different types: Nor, Had and EN. A *normal* value (Nor) is an array (tensor product) of single-qubit values $|0\rangle$ or $|1\rangle$. Sometimes, a (Nor)-typed value is associated with an amplitude z , representing an intermediate partial program state. A *Hadamard* (Had) typed value represents a collection of qubits in superposition but not entangled, i.e., an n -qubit array $\frac{1}{\sqrt{2}}(|0\rangle + \alpha(r_0)|1\rangle) \otimes \dots \otimes \frac{1}{\sqrt{2}}(|0\rangle + \alpha(r_{n-1})|1\rangle)$, can be encoded as $\frac{1}{\sqrt{2^n}} \otimes_{j=0}^{n-1} (|0\rangle + \alpha(r_j)|1\rangle)$, with $\alpha(r_j) = e^{2\pi i r_j}$ ($r_j \in \mathbb{R}$) being the *local phase*, a special amplitude whose norm is 1, i.e., $|\alpha(r_j)| = 1$. The most general form of n -qubit values is the *entanglement* (EN) typed value, consisting of a linear combination (represented as an array) of basis-kets, as $\sum_{j=0}^m z_j \beta_j \eta_j$, where m is the number of elements in the array. In DisQ, we *extend* traditional basis-ket structures in the Dirac notation to be the above form, so each basis-ket of the above value contains not only an amplitude z_j and a basis β_j but also a frozen basis stack η_j , storing bases not directly involved in the current computation. Here, β_j can always be represented as a single $|c_j\rangle$ by the equation in Figure 3. Every β_j in the array has the same cardinality, e.g., if $|c_0| = n$ ($\beta_0 = |c_0\rangle$), then $|c_i| = n$ ($\beta_j = |c_j\rangle$) for all j .

In DisQ, a locus represents a possibly entangled qubit group. From the study of many quantum algorithms [Ambainis 2004; Beauregard 2003; Childs et al. 2007; Häner et al. 2017; Magniez et al. 2005; Nielsen and Chuang 2011; Rigolin 2005; Shor 1994], we found that the establishment of an entanglement group can be viewed as a loop structure of incrementally adding a qubit to the group at a time, representing the entanglement's scope expansion. This behavior is similar to splits and joins of array elements if we view quantum states as arrays. However, joining and splitting two

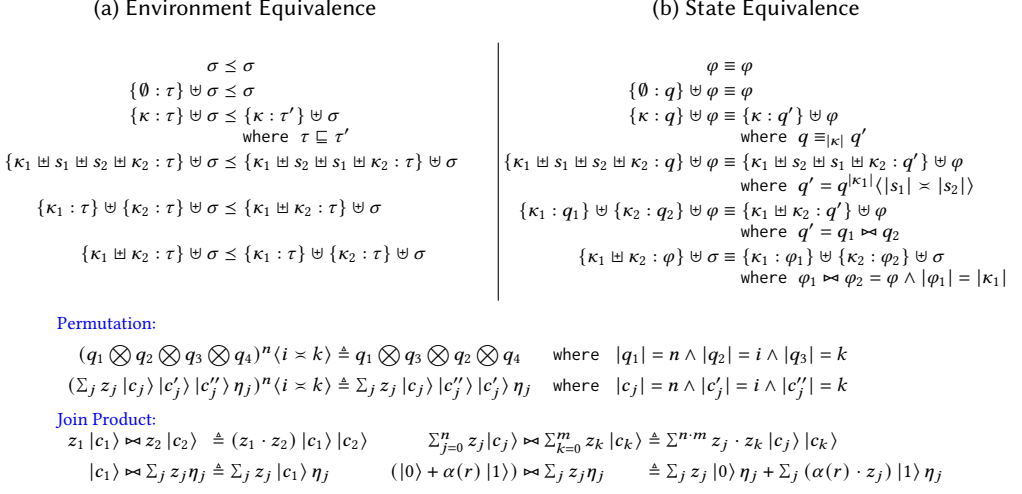


Fig. 13. DisQ type/state relations. \cdot is math mult. Term $\Sigma^{n+m} P$ is a summation omitting the indexing details. \otimes expands a Had array, as $\frac{1}{\sqrt{2^{n+m}}} \otimes_{j=0}^{n+m-2} q_j = (\frac{1}{\sqrt{2^n}} \otimes_{j=0}^{n-1} q_j) \otimes (\frac{1}{\sqrt{2^m}} \otimes_{j=0}^{m-1} q_j)$.

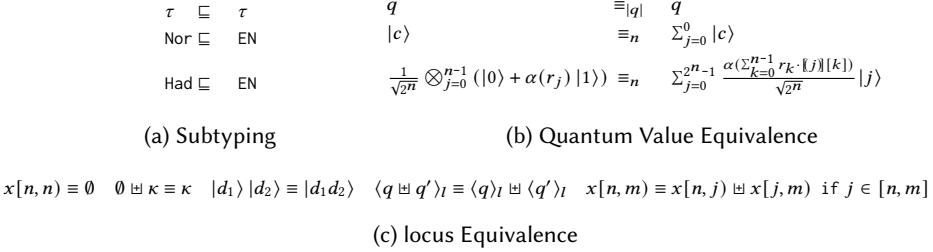


Fig. 14. DisQ type/state relations.

EN-typed values are hard problems³. Another critical observation in studying many quantum algorithms is that the entanglement group establishment usually involves splitting a qubit in a Nor/Had typed value and joining it to an existing EN typed entanglement group. We manage these join and split patterns type-guided equations in DisQ, suitable for automated verification.

The semantics in Figure 6 assumes that the loci in quantum states can be in ideal forms, e.g., rule S-OP assumes that the target locus κ are always prefixed. This step is valid if we can rewrite (type environment partial order \leq) the locus to the ideal form through rule T-PAR and T-PARM in Figure 8, which interconnectively rewrites the locus appearing in the state, through our state equivalence relation (\equiv), as the locus state simultaneity enforcement. The state equivalence rewrites have two components.

First, the type and quantum value forms have simultaneity in Figure 14, i.e., given a type τ_1 for a locus κ in a type environment (Σ), if it is a subtype (\sqsubseteq) of another type τ_2 , K 's value q_1 in a state (Φ) can be rewritten to q_2 that has the type τ_2 through state equivalence rewrites (\equiv_n) where n is the number of qubits in q_1 and q_2 . Both \sqsubseteq and \equiv_n are reflexive and types Nor and Had are subtypes

³The former is a Cartesian product; the latter is $\geq NP$ -hard.

of EN, which means that a Nor typed value ($|c\rangle$) and a Had typed value ($\frac{1}{\sqrt{2^n}} \otimes_{j=0}^{n-1} (|0\rangle + \alpha(r_j) |1\rangle)$) can be rewritten to an EN typed value. For example, a Had typed value $\frac{1}{\sqrt{2^n}} \otimes_{j=0}^{n-1} (|0\rangle + |1\rangle)$ can be rewritten to an EN type as $\sum_{i=0}^{2^n-1} \frac{1}{\sqrt{2^n}} |i\rangle$. If such a rewrite happens, we correspondingly transform $x[0, n]$'s type to EN in the type environment.

Second, type environment partial order (\leq) and state equivalence (\equiv) also have simultaneity in Figure 13 for local loci, and the relations between loci can be derived based on the following rules, as well as permutations on \boxplus operations.

$$\frac{\sigma \leq \sigma'}{\langle \sigma \boxplus \sigma_1 \rangle_l \boxplus \Sigma \leq \langle \sigma' \boxplus \sigma_1 \rangle_l \boxplus \Sigma} \qquad \frac{\varphi \leq \varphi'}{\langle \varphi \boxplus \varphi_1 \rangle_l \boxplus \Phi \leq \langle \varphi' \boxplus \varphi_1 \rangle_l \boxplus \Phi}$$

Here, we associate a state Φ , with the type environment Σ by sharing the same domain, i.e., $\text{dom}(\Phi) = \text{dom}(\Sigma)$. Thus, the environment rewrites (\leq) happening in Σ gear the state rewrites in Φ . In Figure 13, the rules of environment partial order and state equivalence are one-to-one corresponding. The first three lines describe the properties of reflective, identity, and subtyping equivalence. The fourth line enforces that the environment and state are close under locus permutation. After the equivalence rewrite, the position bases of ranges s_1 and s_2 are mutated by applying the function $q^{|\kappa_1|} \langle |s_1| \succ |s_2| \rangle$. One example is the following local locus rewrite from left to right, where we permute the two ranges $x[0, n]$ and $y[0, n]$.

$$\begin{aligned} \{x[0, n] \boxplus y[0, n] : \text{EN}\} &\leq \{y[0, n] \boxplus x[0, n] : \text{EN}\} \\ \{x[0, n] \boxplus y[0, n] : \sum_{i=0}^{2^n-1} \frac{1}{\sqrt{2^n}} |i\rangle |a^i \% N\rangle\} &\equiv \{y[0, n] \boxplus x[0, n] : \sum_{i=0}^{2^n-1} \frac{1}{\sqrt{2^n}} |a^i \% N\rangle |i\rangle\} \end{aligned}$$

The last two lines in Figures 13a and 13b describe locus joins and splits, where the latter is an inverse of the former but much harder to perform practically. In the most general form, joining two EN-type states computes the Cartesian product of their basis-kets, shown in the bottom of Figure 13; such operations are computational expensive in verification and validation. Fortunately, the join operations in most quantum algorithms are between a Nor/Had typed and an EN-typed state, Joining a Nor-typed and EN-typed state puts extra qubits in the right location in every basis-ket of the EN-typed state.

C WELL-FORMEDNESS

The correctness of our type system in Section 5.2 is assumed to have well-formed domains below.

Definition C.1 (Well-formed locus domain). The domain of a environment Σ (or state Φ) is *well-formed*, written as $\Omega \vdash \text{dom}(\Sigma)$ (or $\text{dom}(\Phi)$), iff for every locus $\kappa \in \text{dom}(\Sigma)$ (or $\text{dom}(\Phi)$):

- K is disjoint unioned, for every $\kappa \in K$, and for every two ranges $x[i, j]$ and $y[i', j']$ in κ , $x[i, j] \cap y[i', j'] = \emptyset$.
- For every $\kappa \in K$, and for every range $x[i, j] \in \kappa$, $\Omega(x) = Q(n)$ and $[i, j] \subseteq [0, n]$.

Besides well-formed domain definition, we also require that states (Φ) being well-formed ($\Omega; \Sigma \vdash \Phi$), defined as follows. Here, we use $\Sigma(K)$ and $\Phi(K)$ to find the corresponding state entry pointed to by a locus K' , such that there exists $K_1 \cdot K' = K \boxplus K_1$.

Definition C.2 (Well-formed DisQ state). A state Φ is *well-formed*, written as $\Omega; \Sigma \vdash \Phi$, iff $\text{dom}(\Sigma) = \text{dom}(\Phi)$, $\Omega \vdash \text{dom}(\Sigma)$ (all variables in Φ are in Ω), and:

- For every $K \in \text{dom}(\Sigma)$, s.t. $\Sigma(K) = \text{Nor}$, $\Phi(K) = z |c\rangle \langle \beta|$ and $|\kappa| = |c|$ and $|z| \leq 1$; specifically, if $g = C$, $\beta = \emptyset$ and $|z| = 1$.⁴
- For every $K \in \text{dom}(\Sigma)$, s.t. $\Sigma(K) = \text{Had}$, $\Phi(K) = \frac{1}{\sqrt{2^n}} \otimes_{j=0}^{n-1} (|0\rangle + \alpha(r_j) |1\rangle)$ and $|K| = n$.

⁴ $|K|$ and $|c|$ are the lengths of K and c , and $|z|$ is the norm.

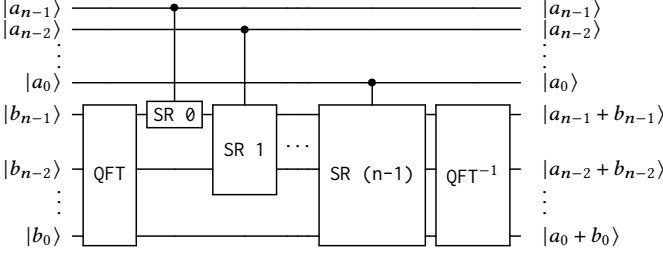


Fig. 15. Quantum QFT-Based Adder Circuit

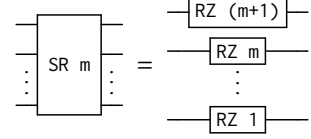


Fig. 16. SR unfolds to many RZ gates.

- For every $K \in \text{dom}(\Sigma)$, s.t. $\Sigma(K) = \text{EN}$, $\Phi(K) = \sum_{j=0}^m z_j |c_j\rangle \langle \beta_j|$, and for all j , $|K| = |c_j|$ and $\sum_{j=0}^m |z|^2 \leq 1$; specifically, if $g = \text{C}$, for all j , $\beta_j = \emptyset$ and $\sum_{j=0}^m |z|^2 = 1$.

D DISTRIBUTED QFT ADDER

A QFT-based adder (Figure 15) performs addition differently than a ripple-carry adder. It usually comes with two qubit arrays y and u , tries to sum the y bits into the u array, by first transforming u 's qubits to QFT-basis and performing addition in the basis, i.e., instead of performing bit arithmetic in a ripple-carry adder, it records addition results via phase rotations. The final inversed QFT operation QFT^{-1} transforms the addition result in the qubit phase back to basis vectors. We show the distributed version of a QFT-adder below, which has a different way of distribution than the ripple-carry adder above.

Example D.1 (Distributed QFT Adder). We define the adder as the membrane definition below. Membrane l holds qubit array x and membrane r takes care of qubit array y , and they share two n -qubit quantum channels c and c' . C-SR(j) is the controlled SR operation, where $c[j] \boxplus y[0, n] \leftarrow \text{C-SR}(j)$ means controlling over $c[j]$ on applying SR to the $y[0, n]$ range.

Recursive Combinator:

$$\text{Rec}(j, n, f) = \text{if } (j = n) \ 0 \ \text{else } f(j) . \text{Rec}(j+1)$$

Process Definitions:

$$\begin{aligned} \text{Se}(j) &= \text{Te}(x[j], c[j]) . \text{Rt}(c'[j]) & \text{SeR}(n) &= \text{Rec}(0, n, \text{Se}) \\ \text{Re}(j) &= \text{Rt}(c[j]) . c[j] \boxplus y[0, n] \leftarrow \text{C-SR}(j) . \text{Te}(c[j], c'[j]) & \text{ReR}(n) &= \text{Rec}(0, n, \text{Re}) \end{aligned}$$

Membrane Definition:

$$\partial c(n) . \partial c'(n) . \{\text{SeR}(n)\}_l, \partial c(n) . \partial c'(n) . \{y[0, n] \leftarrow \text{QFT} . \text{ReR}(n) . y[0, n] \leftarrow \text{QFT}^{-1} . 0\}_r$$

In the above example, after the two n -qubit quantum channel (c and c') are created, membrane r transforms qubit array y to be in QFT-basis. The loop in membrane l sends a qubit in the x array at a time to membrane r via a single qubit quantum channel in c . In the j -th iteration, membrane r receives the information in the qubit $x[j]$, stored in $\langle c[j] \rangle_r$, and applies a C-SR operation that controls over the qubit $\langle c[j] \rangle_r$ on applying SR operation on the y qubit array. Assume that the qubit state in $x[j]$ is $|d_j\rangle$ ($d_j = 0$ or $d_j = 1$), the controlled SR operation adds $2^j * d_j$ to array y 's phase by performing a series of RZ rotations. Then, we teleport $c[j]$ back to membrane l via another single qubit quantum channel in c' . After the loop, we apply an inversed QFT gate to transform the addition result in y 's phase back to its basis vectors.

In each integration, after membrane l teleports qubit $x[j]$ to membrane r , as well as membrane r teleports qubit $c[j]$ to $c'[j]$ in membrane l , the $x[j]$ and $c[j]$ qubits are destroyed, so the qubit numbers in membranes l and r are always less than n and $n+1$, respectively.